

Semimartingale and continuous-time Markov chain approximation for rough stochastic local volatility models ^{*}

Jingtang Ma,[†] Wensheng Yang[‡] and Zhenyu Cui[§]

November 1, 2021

Abstract

Rough volatility models have recently been empirically shown to provide a good fit to historical volatility time series and implied volatility smiles of SPX options. They are continuous-time stochastic volatility models, whose volatility process is driven by a fractional Brownian motion with Hurst parameter less than half. Due to the challenge that it is neither a semimartingale nor a Markov process, there is no unified method that not only applies to all rough volatility models, but also is computationally efficient. This paper proposes a semimartingale and continuous-time Markov chain (CTMC) approximation approach for the general class of rough stochastic local volatility (RSLV) models. In particular, we introduce the perturbed stochastic local volatility (PSLV) model as the semimartingale approximation for the RSLV model and establish its existence, uniqueness and Markovian representation. We propose a fast CTMC algorithm and prove its weak convergence. Numerical experiments demonstrate the accuracy and high efficiency of the method in pricing European, barrier and American options. Comparing with existing literature, a significant reduction in the CPU time to arrive at the same level of accuracy is observed.

JEL classification: C63, G13

Keywords: Continuous-time Markov chain, rough stochastic local volatility models, semimartingale approximation, option pricing

1 Introduction

Recently, a new class of stochastic volatility model, named the *rough volatility* model, was proposed in Gatheral et al. (2018), and has since then generated significant amount of interests from both academia and industry. The key insight of this model is to assume that

^{*}The work was supported by National Natural Science Foundation of China (Grant No. 12071373) and the Fundamental Research Funds for the Central Universities China (JBK1805001). We would like to thank Antoine Jacquier and Philipp Schoenbauer for discussions leading to improvement in the paper.

[†]School of Economic Mathematics, Southwestern University of Finance and Economics, Chengdu, 611130, P.R. China (Email: mjt@swufe.edu.cn).

[‡]School of Economic Mathematics, Southwestern University of Finance and Economics, Chengdu, 611130, P.R. China (Email: yangws@swufe.edu.cn).

[§]Corresponding author. School of Business, Stevens Institute of Technology, Hoboken, New Jersey 07030, United States. (Email: zcui6@stevens.edu).

the latent stochastic volatility process is driven by a fractional Brownian motion, in contrast to a standard Brownian motion (e.g. in traditional stochastic (local) volatility models). The trajectories of the volatility process are continuous but exhibit irregular path properties due to the fractional Brownian motion driver. From empirical studies, [Gatheral et al. \(2018\)](#) find that the log-volatility essentially behaves like a fractional Brownian motion with Hurst exponent H of order 0.1, at any reasonable time scale. Further empirical evidence has been documented in [Fukasawa et al. \(2019\)](#), where the authors constructed a quasi-likelihood estimator applied to realized volatility time series, and confirmed that the Hurst parameter is much smaller than half, i.e. volatility is indeed rough.

The rough volatility model has enjoyed huge success in reproducing many stylized facts of historical volatility time series and implied volatility smiles for SPX options. On one hand, rough volatility models provide remarkably accurate fit to the shape of implied volatility smiles, and in particular for at-the-money skew curves. They also reproduce stylized facts for realized volatilities ([El Euch et al., 2019](#); [Livieri et al., 2018](#)). On the other hand, it is consistent with economic micro-structural models and naturally emerges from economic agents' behaviors, as shown in [El Euch et al. \(2018\)](#). It also has intrinsic connections with Hawkes processes, see [Jaisson and Rosenbaum \(2016\)](#); [Dandapani et al. \(2021\)](#).

The existence of the fractional kernel forces the variance process to leave both the semi-martingale and Markovian worlds, hence one important yet challenging problem in the rough volatility research is to find an efficient and accurate method to evaluate derivative prices, whereas closed-form formulae are in general not available. On one hand, several analytical approximation methods have been introduced and studied in [Forde and Zhang \(2017\)](#); [Guenoun et al. \(2018\)](#); [Forde et al. \(2021b\)](#). On the other hand, the Monte Carlo simulation of rough volatility model has been studied in [Bayer et al. \(2016\)](#); [Forde et al. \(2021a\)](#), etc. Due to the memory in the volatility process, the Monte Carlo simulation of rough volatility process is very time consuming, and there is recent research on improving its efficiency, see [McCrickerd et al. \(2018\)](#); [Bayer et al. \(2020\)](#); [Ma and Wu \(2021\)](#). In the special class of affine rough volatility models, one is able to price options through Fourier transform based methods by utilizing the characteristic function via solving fractional Riccati systems. In particular, [El Euch and Rosenbaum \(2019\)](#) generalized the classical Heston model to the rough Heston model and derive the characteristic function of the log asset price. See also [Abi Jaber and El Euch \(2019b\)](#); [Richard et al. \(2021\)](#); [Abi Jaber and El Euch \(2019a\)](#) for extensions. Note that some numerical challenges still remain for solving the fractional Riccati system in an efficient way, and see [Callegaro et al. \(2021\)](#) for recent developments along that direction. In general, without the affine structure, the characteristic function for the rough volatility model is not available.

In general, the Monte Carlo method has low computational efficiency, and the method of finding the characteristic function is not suitable for all rough volatility models outside of the special class of affine rough volatility models. Inspecting the existing literature¹, to the best of authors' knowledge, there is no method that is not only generally applicable to various rough volatility models but also has good accuracy and computational efficiency. This motivates us to search for a general method that is widely applicable to the broad class of rough stochastic local volatility (RSLV) models (see equation (1)). Inspired by the recent success on using the continuous-time Markov chain (CTMC) method in derivatives pricing (see the survey [Cui et al. \(2019\)](#) and references therein), this paper aims to extend

¹There is a website dedicated to collecting the most up-to-date literature on rough volatility research: <https://sites.google.com/site/roughvol/home/risks-1>

the applicability of the CTMC method to the realm of rough volatility models for the first time.

Our method comprises of two main steps. The first step is a novel semimartingale approximation to the RSLV model, and we obtain the “perturbed stochastic local volatility (PSLV) model”, which is new to the literature. This removes the singularity in the kernel function. The second step is the CTMC approximation to the PSLV model, and we manage to obtain an explicit formula involving matrix expressions. In the first step above, we provide a new semimartingale approximation to the general class of RSLV models, which is of independent theoretical interest. It is important to distinguish this semimartingale approximation from a recent series of literature on the Markovian approximation to rough volatility models, which started from [Abi Jaber and El Euch \(2019c\)](#), [Alfonsi and Kebaier, \(2021\)](#), and see also [Harms \(2019\)](#) for the case of fractional Brownian motion. The main idea there is to represent the fractional process as an integral over a family of Ornstein-Uhlenbeck processes, and then apply numerical discretization (i.e. quadrature) to the integral. The final result is a $(n + 2)$ -dimensional stochastic differential equation system, where n is the number of grid points of numerical integration. In contrast, our approach is based on the perturbation idea, which was first introduced in [Dung \(2011\)](#) for the case of fractional Brownian motions, and we extend it to the case of general RSLV models to arrive at the PSLV model. The final result is a stochastic differential equation system, and the stochastic volatility process in this system is a semimartingale and Markov process. See Remark 2.4.

The contributions of this paper are three-fold:

1. This paper extends the traditional stochastic local volatility (SLV) model to the rough version, and names it the rough stochastic local volatility (RSLV) model. Using the semimartingale approximation to the RSLV model, a new model named the “perturbed stochastic local volatility” (PSLV) model, and its stochastic differential form are obtained. In addition, this paper discusses the existence, uniqueness, regularity, semimartingale property and the Markov property of the PSLV model, and also prove that it converges weakly to the original RSLV model.
2. A novel CTMC approximation method is developed, and we express options prices under the RSLV model in explicit matrix formulae. To the best of authors’ knowledge, this is the first CTMC algorithm designed for the RSLV model. Theoretical convergence of this algorithm is established. In addition, a fast algorithm (Algorithm 5.1) for pricing European and barrier option is given. Compared with the traditional coupled two-dimensional CTMC method ([Cui et al., 2018](#)), the new CTMC algorithm is decoupled. There is a significant improvement in computer storage space and computing capacity (see Remark 5.1).
3. Numerical examples demonstrate the accuracy and high efficiency of our method. In particular, the method can deliver European and barrier options prices up to 3 digits of accuracy in 0.18 seconds of CPU time. Note that the method is universally fast and accurate across all RSLV models, and it is applicable not only to path-independent options such as European call/put options, but also to path-dependent options such as barrier options and American options. There is a significant reduction in the CPU time to arrive at the same level of accuracy, as compared to benchmark methods in the literature.

The remainder of this paper is organized as follows. Section 2 presents the new PSLV

model, studies its properties, proves its convergence to the RSLV model and provides its Markovian representation. Section 3 gives the CTMC approximation and establishes its weak convergence. Section 4 considers the European, barrier and American options pricing problems under the RSLV model and gives the explicit matrix expressions for their prices. Numerical experiments are reported in Section 5. Finally, Section 6 concludes the paper.

2 Semimartingale approximation of rough stochastic local volatility models

2.1 Rough stochastic local volatility models

We consider the asset price $\{S_t : t \in \mathbb{T}\}$ with $\mathbb{T} := [0, T]$ which is defined on a filtered probability space $(\Omega, \mathcal{F}, \mathbb{F}, \mathbb{P})$, where $\mathbb{F} = \{\mathcal{F}_t\}_{t \geq 0}$ denotes the standard filtration generated by a two-dimensional \mathbb{F} -Brownian motion (B, B^\perp) and $W = \rho B + \sqrt{1 - \rho^2} B^\perp$ with constant correlation $\rho \in (-1, 1)$. We first recall the classical stochastic local volatility (SLV) model as follows

$$\text{SLV: } \begin{cases} dS_t = \mu(S_t, V_t)dt + \varphi(V_t)\nu(S_t)dW_t, \\ dV_t = b(V_t)dt + \sigma(V_t)dB_t, \end{cases}$$

where $\mu(\cdot, \cdot) : \mathbb{R} \times \mathbb{R} \rightarrow \mathbb{R}$, $\varphi(\cdot) : \mathbb{R} \rightarrow \mathbb{R}_+$, $\nu(\cdot) : \mathbb{R} \rightarrow \mathbb{R}_+$, $b(\cdot) : \mathbb{R} \rightarrow \mathbb{R}$, $\sigma(\cdot) : \mathbb{R} \rightarrow \mathbb{R}_+$. W_t and B_t are two Brownian motions with a constant correlation $\rho \in (-1, 1)$, that is, $E[dW_t dB_t] = \rho dt$. The SLV model nests several representative models in the literature as special cases, such as Heston (Heston, 1993), 4/2 (Grasselli, 2017), Stein-Stein (Stein and Stein, 1991), 3/2 (Lewis, 2000), Hull-White (Hull and White, 1987), α -Hypergeometric (Da Fonseca and Martini, 2016), SABR² (Hagan et al., 2002), Heston-SABR (Van der Stoep et al., 2014), Quadratic SLV (Lipton, 2002), etc.

Recasting the classical SLV model into its rough correspondent, we have the following definition of the rough stochastic local volatility (RSLV) model.

Definition 2.1 (rough stochastic local volatility model) *Under the risk-neutral measure, assume that the underlying asset price S_t follows a rough stochastic local volatility (RSLV) model characterized by the following two-dimensional diffusion system:*

$$\text{RSLV: } \begin{cases} dS_t = \mu(S_t, V_t)dt + \varphi(V_t)\nu(S_t)dW_t, \\ V_t = V_0 + \int_0^t K(t, s) (b(V_s)ds + \sigma(V_s)dB_s), \end{cases} \quad (1)$$

where $K(t, s) := \frac{(t-s)^{H-\frac{1}{2}}}{\Gamma(H+\frac{1}{2})}$ is the fractional kernel with the Hurst parameter $H \in (0, 1/2)$.

In order to ensure the strong existence of continuous solutions to (1), the following regularity assumption is necessary.

Assumption 2.1 $\mu(\cdot, \cdot) : \mathbb{R} \times \mathbb{R} \rightarrow \mathbb{R}$, $\nu(\cdot) : \mathbb{R} \rightarrow \mathbb{R}_+$, $b(\cdot) : \mathbb{R} \rightarrow \mathbb{R}$, $\varphi(\cdot) : \mathbb{R} \rightarrow \mathbb{R}_+$, $\sigma(\cdot) : \mathbb{R} \rightarrow \mathbb{R}_+$ are all Lipschitz continuous functions with linear growth.

Proposition 2.1 *Under Assumption 2.1, the equation system (1) admits a unique strong continuous solution. Moreover V_t and S_t satisfies*

$$\sup_{t \in \mathbb{T}} \mathbb{E}[|V_t|^p] < \infty, \quad \sup_{t \in \mathbb{T}} \mathbb{E}[|S_t|^p] < \infty, \quad p > 0.$$

In addition, V and S admit Hölder continuous paths on \mathbb{T} of any order strictly less than H .

²Stochastic Alpha Beta Rho

Proof We refer to [Abi Jaber and El Euch \(2019a\)](#) for the proofs. \square

Remark 2.1 *This paper focuses on kernel function of the following form $K(t, s) = \frac{(t-s)^{H-\frac{1}{2}}}{\Gamma(H+\frac{1}{2})}$. However, under certain assumptions, the method in this paper can be applied directly to a more general class of kernel functions. We refer to [Abi Jaber and El Euch \(2019a\)](#) for discussions on the regularity condition of the kernel function.*

It is well known that the fractional kernel forces the variance process to leave both the semimartingale and Markovian worlds, which makes numerical approximation procedures a difficult and challenging task in practice. [Abi Jaber and El Euch \(2019c\)](#) use a multi-factor model to perform a Markovian approximation to RSLV. We now show an alternative approach to approximate RSLV by a semimartingale model through a perturbation idea.

2.2 Semimartingale approximation

Inspired by [Dung \(2011\)](#), who performs a semimartingale approximation to the fractional Brownian motion, we approximate the fractional kernel $K(t, s)$ by a perturbed kernel $K(t - \varepsilon, s)$ with $0 < \varepsilon \ll 1$. This leads to the following approximation process V_t^ε of the variance process V_t :

$$V_t^\varepsilon := V_0^\varepsilon + \int_0^t K(t + \varepsilon, s) (b(V_s^\varepsilon) ds + \sigma(V_s^\varepsilon) dB_s), \quad V_0^\varepsilon = V_0,$$

where

$$K(t + \varepsilon, s) = \frac{(t + \varepsilon - s)^{H-\frac{1}{2}}}{\Gamma(H + 1/2)}.$$

Remark 2.2 *The original kernel function $K(t, s)$ is singular at the point $s = t$, and the kernel function $K(t + \varepsilon, s)$ obtained by the semimartingale approximation is smooth for any $s \in [0, t]$.*

The first lemma establishes the semimartingale property of the process V_t^ε .

Lemma 2.1 *For any $\varepsilon > 0$, V_t^ε is a \mathcal{F}_t -semimartingale with decomposition*

$$V_t^\varepsilon = V_0^\varepsilon + \int_0^t (K(t + \varepsilon, s)b(V_s^\varepsilon) + \psi_s^\varepsilon) ds + \int_0^t K(s + \varepsilon, s)\sigma(V_s^\varepsilon)dB_s, \quad (2)$$

where

$$\psi_s^\varepsilon := \int_0^s \partial_1 K(s + \varepsilon, u)\sigma(V_u^\varepsilon)dB_u, \quad \partial_1 K(s + \varepsilon, u) = \frac{(H - \frac{1}{2})(s + \varepsilon - u)^{H-\frac{3}{2}}}{\Gamma(H + \frac{1}{2})}.$$

Proof The lemma follows from a straightforward application of the stochastic Fubini theorem (c.f. Theorem 2.2 in [Veraar \(2012\)](#)):

$$\begin{aligned} \int_0^t \psi_s^\varepsilon ds &= \int_0^t \int_0^s \partial_1 K(s + \varepsilon, u)\sigma(V_u^\varepsilon)dB_u ds \\ &= \int_0^t \left(\int_u^t \partial_1 K(s + \varepsilon, u) ds \right) \sigma(V_u^\varepsilon)dB_u \\ &= \int_0^t (K(t + \varepsilon, u) - K(u + \varepsilon, u))\sigma(V_u^\varepsilon)dB_u \\ &= \int_0^t K(t + \varepsilon, s)\sigma(V_s^\varepsilon)dB_s - \int_0^t K(s + \varepsilon, s)\sigma(V_s^\varepsilon)dB_s. \end{aligned}$$

This completes the proof. \square

The second lemma establishes the strong existence and uniqueness of V_t^ε .

Lemma 2.2 *Under Assumption 2.1, for any $\varepsilon > 0$, there exists a unique strong solution V_t^ε . Moreover V_t^ε satisfies*

$$\sup_{t \in \mathbb{T}} \mathbb{E}[|V_t^\varepsilon|^p] < \infty, \quad p > 0,$$

and admits Hölder continuous paths on \mathbb{T} of any order strictly less than H .

Proof We first prove the existence of V_t^ε . Thanks to the continuity of $K(t + \varepsilon, s)$ and boundedness of $\partial_1 K(t + \varepsilon, s) = \frac{(H-1/2)(t+\varepsilon-s)^{H-3/2}}{\Gamma(H+1/2)}$, the proof of Theorems 3.3 and 3.4 in [Abi Jaber and El Euch \(2019a\)](#) can be directly applied to prove the existence of V_t^ε . Now we show the pathwise uniqueness. Since V_t^ε is a semimartingale as shown in Lemma 2.1 and $K(t + \varepsilon, t) = \frac{\varepsilon^{H-\frac{1}{2}}}{\Gamma(H+1/2)} < \infty$, we can use a similar proof as that of Proposition B.3. in [Abi Jaber and El Euch \(2019c\)](#) to establish the uniqueness of V_t^ε . This completes the proof. \square

The next theorem proves the convergence of the semimartingale approximation.

Theorem 2.1 *Under Assumption 2.1, the process V_t^ε converges to V_t in $\mathbf{L}^2(\Omega, \mathbb{T})$ as ε tends to 0, uniformly in $t \in \mathbb{T}$.*

Proof

$$\begin{aligned} & E[|V_t^\varepsilon - V_t|^2] \\ &= E \left[\left| \int_0^t K(t + \varepsilon, s)(b(V_s^\varepsilon) - b(V_s))ds + \int_0^t (K(t + \varepsilon, s) - K(t, s))b(V_s)ds \right. \right. \\ & \quad \left. \left. + \int_0^t K(t + \varepsilon, s)(\sigma(V_s^\varepsilon) - \sigma(V_s))dB_s + \int_0^t (K(t + \varepsilon, s) - K(t, s))\sigma(V_s)dB_s \right|^2 \right]. \end{aligned}$$

Recalling the power mean inequality: for $k \geq 1, x_1, x_2, \dots, x_\ell \geq 0, \ell \in \mathbb{N}_+, \sum_{i=1}^\ell \frac{x_i}{\ell} \leq (\sum_{i=1}^\ell \frac{x_i^k}{\ell})^{1/k}$ and using Itô isometry and the Cauchy-Schwarz's inequality, we have

$$\begin{aligned} & E[|V_t^\varepsilon - V_t|^2] \\ & \leq 4E \left[\left(\int_0^t K(t + \varepsilon, s)(b(V_s^\varepsilon) - b(V_s))ds \right)^2 + \left(\int_0^t (K(t + \varepsilon, s) - K(t, s))b(V_s)ds \right)^2 \right. \\ & \quad \left. + \int_0^t K^2(t + \varepsilon, s)(\sigma(V_s^\varepsilon) - \sigma(V_s))^2 ds + \int_0^t (K(t + \varepsilon, s) - K(t, s))^2 \sigma^2(V_s) ds \right] \\ & \leq 4E \left[\int_0^t K^2(t + \varepsilon, s) \left(t(b(V_s^\varepsilon) - b(V_s))^2 + (\sigma(V_s^\varepsilon) - \sigma(V_s))^2 \right) ds \right. \\ & \quad \left. + \int_0^t (K(t + \varepsilon, s) - K(t, s))^2 (tb^2(V_s) + \sigma^2(V_s)) ds \right]. \end{aligned}$$

By the conditions that b, σ are Lipschitz continuous with linear growth, and the stochastic Fubini theorem, we have

$$\begin{aligned} E[|V_t^\varepsilon - V_t|^2] & \leq 4 \left(C_1(1+t) \int_0^t K^2(t + \varepsilon, s) E[|V_s^\varepsilon - V_s|^2] ds \right. \\ & \quad \left. + \int_0^t (K(t + \varepsilon, s) - K(t, s))^2 C_1(1+t)(1 + E[|V_s|] + E[V_s^2]) ds \right). \end{aligned}$$

Here and throughout this paper, we use C_i , $i = 1, 2, \dots$, to represent positive constants. By Taylor expansion, there is

$$K(t + \varepsilon, s) - K(t, s) = \frac{(t + \varepsilon - s)^{H - \frac{1}{2}} - (t - s)^{H - \frac{1}{2}}}{\Gamma(H + 1/2)} = \varepsilon \frac{(H - \frac{1}{2})(t + \varepsilon - s)^{H - \frac{3}{2}}}{\Gamma(H + 1/2)} + o(\varepsilon),$$

and $E[|V_s|^p] < \infty$ for $p > 0$ from Proposition 2.1, then we obtain

$$\begin{aligned} & \int_0^t \left[(K(t + \varepsilon, s) - K(t, s))^2 C(1 + t)(1 + E[|V_s|] + E[V_s^2]) \right] ds \\ & \leq C_2 \int_0^t \left(\varepsilon \frac{(H - \frac{1}{2})(t + \varepsilon - s)^{H - \frac{3}{2}}}{\Gamma(H + 1/2)} + o(\varepsilon) \right) ds = C_2 \varepsilon^{H + \frac{1}{2}} + \mathcal{O}(\varepsilon). \end{aligned}$$

Finally, using Grönwall's inequality leads to

$$\begin{aligned} E[|V_t^\varepsilon - V_t|^2] & \leq 4 \left[C_1(1 + t) \int_0^t K^2(t + \varepsilon, s) E[|V_s^\varepsilon - V_s|^2] ds + C_2 \varepsilon^{H + \frac{1}{2}} + \mathcal{O}(\varepsilon) \right] \\ & \leq C_3 \varepsilon^{H + \frac{1}{2}}. \end{aligned}$$

This completes the proof. \square

Given the existence, uniqueness, semimartingale and convergence properties of V_t^ε , we now define the so-called perturbed stochastic local volatility (PSLV) model $(S_t^\varepsilon, V_t^\varepsilon)$, which serves as an approximation of (S_t, V_t) .

Definition 2.2 (perturbed stochastic local volatility models) *We define the following stochastic local volatility model $(S_t^\varepsilon, V_t^\varepsilon)$ with perturbation parameters $0 < \varepsilon \ll 1$ as the unique strong solution of*

$$PSLV: \quad \begin{cases} dS_t^\varepsilon = \mu(S_t^\varepsilon, V_t^\varepsilon) dt + \varphi(V_t^\varepsilon) \nu(S_t^\varepsilon) dW_t, \\ V_t^\varepsilon = V_0^\varepsilon + \int_0^t K(t + \varepsilon, s) (b(V_s^\varepsilon) ds + \sigma(V_s^\varepsilon) dB_s), \quad V_0^\varepsilon = V_0, \end{cases} \quad (3)$$

under the same filtered probability space $(\Omega, \mathcal{F}, \mathbb{F}, \mathbb{P})$ as (S_t, V_t) defined by (1).

Proposition 2.2 *Under Assumption 2.1, the equation system (3) admits a unique strong continuous solution.*

Proof The strong existence and uniqueness of V_t^ε is given by Lemma 2.2. Moreover, S_t^ε satisfies a stochastic differential equation and there exists an unique strong solution to it under Assumption 2.1 (see e.g., Oksendal (2013)). This completes the proof. \square

As shown in Theorem 2.1, V_t^ε converges to V_t as ε tends to 0. The next theorem shows the convergence of S_t^ε to S_t .

Theorem 2.2 *Under Assumption 2.1, the process S_t^ε converges to S_t in $\mathbf{L}^2(\Omega, \mathbb{T})$ as ε tends to 0, uniformly in $t \in \mathbb{T}$.*

Proof The proof of this theorem is similar to Theorem 2.1. Specifically, using power mean inequality, Itô isometry and the Cauchy-Schwarz's inequality, we obtain

$$\begin{aligned} E[|S_t^\varepsilon - S_t|^2] & \leq 2E \left[\left(\int_0^t (\mu(S_s^\varepsilon, V_s^\varepsilon) - \mu(S_s, V_s)) ds \right)^2 + \int_0^t (\varphi(V_s^\varepsilon) \nu(S_s^\varepsilon) - \varphi(V_s) \nu(S_s))^2 ds \right] \\ & \leq 2E \left[\int_0^t t (\mu(S_s^\varepsilon, V_s^\varepsilon) - \mu(S_s, V_s))^2 ds + \int_0^t (\varphi(V_s^\varepsilon) \nu(S_s^\varepsilon) - \varphi(V_s) \nu(S_s))^2 ds \right]. \end{aligned}$$

Then using the condition that μ , φ and ν are Lipschitz continuous with linear growth, and the stochastic Fubini theorem, we have

$$E[|S_t^\varepsilon - S_t|^2] \leq C_4(1+t) \left(\int_0^t E[|S_s^\varepsilon - S_s|^2] ds + \int_0^t E[|V_s^\varepsilon - V_s|^2] ds \right).$$

Thanks to Theorem 2.1 and Grönwall's inequality, we have

$$E[|S_t^\varepsilon - S_t|^2] \leq C_5 \varepsilon^{H+\frac{1}{2}}.$$

This completes the proof. \square

2.3 Markovian representation of the PSLV model

In the PSLV model (3) obtained by semimartingale approximation, since the singularity of the integral kernel K at point 0 is eliminated, we can prove that V_t^ε is Markovian through the following theorem.

Theorem 2.3 *The stochastic process V_t^ε is a Markov process, and satisfies the following stochastic differential equation:*

$$dV_t^\varepsilon = K^\varepsilon b(V_t^\varepsilon) dt + \varphi_t^\varepsilon dt + K^\varepsilon \sigma(V_t^\varepsilon) dB_t, \quad (4)$$

where

$$K^\varepsilon := K(t + \varepsilon, t)$$

and

$$\varphi_t^\varepsilon := \int_0^t \partial_1 K(t + \varepsilon, u) (b(V_u^\varepsilon) dt + \sigma(V_u^\varepsilon) dB_u), \quad \partial_1 K(t + \varepsilon, u) = \frac{(H - \frac{1}{2})(t + \varepsilon - u)^{H-\frac{3}{2}}}{\Gamma(H + \frac{1}{2})}.$$

Proof Differentiating equation (2), (4) is obtained directly. Now we show the Markovian property of V_t^ε . Integrating from s to t , for $0 \leq s \leq t \leq T$, both sides of the equation (4) gives

$$\begin{aligned} & V_t^\varepsilon - V_s^\varepsilon \\ &= \int_s^t K(u + \varepsilon, u) (b(V_u^\varepsilon) du + \sigma(V_u^\varepsilon) dB_u) + \int_s^t \int_0^u \partial_1 K(u + \varepsilon, \xi) (b(V_\xi^\varepsilon) d\xi + \sigma(V_\xi^\varepsilon) dB_\xi) du \\ &= \int_s^t K(u + \varepsilon, u) (b(V_u^\varepsilon) du + \sigma(V_u^\varepsilon) dB_u) + \int_s^t \int_s^u \partial_1 K(u + \varepsilon, \xi) (b(V_\xi^\varepsilon) d\xi + \sigma(V_\xi^\varepsilon) dB_\xi) du \\ &\quad + \int_s^t \int_0^s \partial_1 K(u + \varepsilon, \xi) (b(V_\xi^\varepsilon) d\xi + \sigma(V_\xi^\varepsilon) dB_\xi) du \\ &= \int_s^t K(u + \varepsilon, u) (b(V_u^\varepsilon) du + \sigma(V_u^\varepsilon) dB_u) + \int_s^t \int_s^u \partial_1 K(u + \varepsilon, \xi) (b(V_\xi^\varepsilon) d\xi + \sigma(V_\xi^\varepsilon) dB_\xi) du \\ &\quad + \int_s^t (K(s + \varepsilon, \xi) - K(\varepsilon, \xi)) (b(V_\xi^\varepsilon) d\xi + \sigma(V_\xi^\varepsilon) dB_\xi). \end{aligned}$$

Thanks to the zero-mean property of the Itô integral and Fubini theorem, there is

$$\begin{aligned} E[V_t^\varepsilon | \mathcal{F}_s] &= E \left[V_s^\varepsilon + \int_s^t \left(K(u + \varepsilon, u) b(V_u^\varepsilon) + \int_s^u \partial_1 K(u + \varepsilon, \xi) b(V_\xi^\varepsilon) d\xi \right. \right. \\ &\quad \left. \left. + (K(s + \varepsilon, u) - K(\varepsilon, u)) b(V_u^\varepsilon) \right) du \middle| \mathcal{F}_s \right]. \end{aligned}$$

According to Theorem 17.2.3 in [Cohen and Elliott \(2015\)](#), we have

$$E[V_t^\varepsilon | \mathcal{F}_s] = E[V_t^\varepsilon | V_s^\varepsilon], \quad \text{for } 0 \leq s \leq t \leq T,$$

and it follows that V_t^ε is a Markov process for $t \in \mathbb{T}$. This completes the proof. \square

Remark 2.3 *It is well known that V_t in the RSLV model (1) is not a Markov process and does not have Itô differential expression. The reason is that the integral kernel satisfies $K(t, t) = \infty$. However, after the semimartingale approximation, V_t^ε in the PSLV model (3), which has a smooth kernel and $K(t + \varepsilon, t) = \frac{\varepsilon^{H-\frac{1}{2}}}{\Gamma(H+1/2)}$ for a fixed $0 < \varepsilon \ll 1$, is a semimartingale, and it also has Ito differential expressions and Markov property.*

Although (4) shows the Itô differential form of V_t^ε , it is not conducive to calculation and simulation because the term ψ_t^ε is still in the Itô integral form. Next, we consider another differential expression. Inspired by [Abi Jaber and El Euch \(2019c\)](#), the perturbed fractional kernel $K(t + \varepsilon, s) = \frac{(t + \varepsilon - s)^{H-\frac{1}{2}}}{\Gamma(H+1/2)}$ can be written as a Laplace transform of a positive measure m :

$$K(t + \varepsilon, s) = \int_0^\infty e^{-\gamma(t + \varepsilon - s)} m(d\gamma), \quad m(d\gamma) = \frac{\gamma^{-H-\frac{1}{2}} d\gamma}{\Gamma(H + 1/2)\Gamma(1/2 - H)}.$$

Then by the stochastic Fubini theorem, we obtain that

$$V_t^\varepsilon = V_0^\varepsilon + \int_0^\infty e^{-\gamma\varepsilon} V_t^{\varepsilon, \gamma} m(d\gamma), \quad (5)$$

where

$$V_t^{\varepsilon, \gamma} := \int_0^t e^{-\gamma(t-s)} (b(V_s^\varepsilon) ds + \sigma(V_s^\varepsilon) dB_s). \quad (6)$$

Theorem 2.4 *The PSLV model (3) can be expressed as the following system stochastic differential equation:*

$$\begin{cases} dS_t^\varepsilon = \mu(S_t^\varepsilon, V_t^\varepsilon) dt + \varphi(V_t^\varepsilon) \nu(S_t^\varepsilon) dW_t, \\ dV_t^\varepsilon = - \left(\int_0^\infty e^{-\gamma\varepsilon} \gamma V_t^{\varepsilon, \gamma} m(d\gamma) \right) dt + K^\varepsilon b(V_t^\varepsilon) dt + K^\varepsilon \sigma(V_t^\varepsilon) dB_t, \\ dV_t^{\varepsilon, \gamma} = (-\gamma V_t^{\varepsilon, \gamma} + b(V_t^\varepsilon)) dt + \sigma(V_t^\varepsilon) dB_t, \end{cases} \quad (7)$$

Proof By Itô's lemma, for fixed γ , we have

$$\begin{aligned} dV_t^{\varepsilon, \gamma} &= d \left(\int_0^t e^{-\gamma(t-s)} (b(V_s^\varepsilon) ds + \sigma(V_s^\varepsilon) dB_s) \right) \\ &= -\gamma \left(\int_0^t e^{-\gamma(t-s)} (b(V_s^\varepsilon) ds + \sigma(V_s^\varepsilon) dB_s) \right) dt + b(V_t^\varepsilon) dt + \sigma(V_t^\varepsilon) dB_t \\ &= (-\gamma V_t^{\varepsilon, \gamma} + b(V_t^\varepsilon)) dt + \sigma(V_t^\varepsilon) dB_t. \end{aligned}$$

From the definition of $V_t^{\varepsilon, \gamma}$ (6), we have

$$\begin{aligned} E[|V_t^{\varepsilon, \gamma}|] &= E \left[\left| \int_0^t e^{-\gamma(t-s)} (b(V_s^\varepsilon) ds + \sigma(V_s^\varepsilon) dB_s) \right| \right] \\ &\leq E \left[\int_0^t e^{-\gamma(t-s)} (|b(V_s^\varepsilon)| ds + |\sigma(V_s^\varepsilon)| dB_s) \right]. \end{aligned}$$

Since $b(\cdot) : \mathbb{R} \rightarrow \mathbb{R}$ and $\sigma(\cdot) : \mathbb{R} \rightarrow \mathbb{R}_+$ are all Lipschitz continuous functions with linear growth and $\sup_{t \in \mathbb{T}} \mathbb{E}[|V_t^\varepsilon|^p] < \infty$, $p > 0$, then by Fubini theorem, we have that

$$E[|V_t^{\varepsilon, \gamma}|] \leq C \int_0^t e^{-\gamma(t-s)} ds = C \frac{1 - e^{-\gamma t}}{\gamma}.$$

We use the Lebesgue dominated convergence theorem to rewrite (5) as

$$\begin{aligned} dV_t^\varepsilon &= \int_0^\infty e^{-\gamma\varepsilon} dV_t^{\varepsilon, \gamma} m(d\gamma) \\ &= - \left(\int_0^\infty e^{-\gamma\varepsilon} \gamma V_t^{\varepsilon, \gamma} m(d\gamma) \right) dt + \int_0^\infty e^{-\gamma\varepsilon} m(d\gamma) b(V_t^\varepsilon) dt + \int_0^\infty e^{-\gamma\varepsilon} m(d\gamma) \sigma(V_t^\varepsilon) dB_t \\ &= - \left(\int_0^\infty e^{-\gamma\varepsilon} \gamma V_t^{\varepsilon, \gamma} m(d\gamma) \right) dt + K^\varepsilon b(V_t^\varepsilon) dt + K^\varepsilon \sigma(V_t^\varepsilon) dB_t. \end{aligned}$$

Note that by comparing with the formula (4), it can be seen that the first term in the right of above formula is actually equal to φ_t^ε in (4) by using Laplace transform to $\partial_1 K(t + \varepsilon, u)$. This completes the proof. \square

Remark 2.4 *Based on the multifactor approximation, similar Itô differential expressions with Markov properties can be obtained under the rough Heston model (see formula (1.4) in [Abi Jaber and El Euch \(2019c\)](#)). It is worth noting that their approximation method obtains an $(n + 2)$ -dimensional model, where n is the number of grid points of numerical integration and the multifactor model converges to the original model as n tends to infinity. In contrast, the approximate process V_t^ε with Markov property can be obtained by the semi-martingale approximation without numerical integration, thereby avoiding the difficulties caused by multi-dimensional problems in simulation and calculation.*

Next we consider how to use the Markov chain approximation methods to solve this stochastic differential equation system.

3 CTMC approximation

In this section, we use the CTMC method introduced in [Mijatović and Pistorius \(2013\)](#) to approximate $(S_t^\varepsilon, V_t^\varepsilon)$ defined in (3) by a continuous-time Markov chain. To simplify the analysis, we first decouple the correlation between the two driving Brownian motions by introducing an auxiliary process X_t^ε in the following lemma.

Lemma 3.1 *Define the functions $g(x) := \int^x \frac{1}{\nu(u)} du$ and $f(x) := \int^x \frac{\varphi(u)}{K^\varepsilon \sigma(u)} du$. Then the dynamics in (3) can be rewritten as*

$$\begin{cases} dX_t^\varepsilon = \theta(X_t^\varepsilon, V_t^\varepsilon) dt + \sqrt{1 - \rho^2} \varphi(V_t^\varepsilon) dB_t^\perp, \\ dV_t^\varepsilon = - \left(\int_0^\infty e^{-\gamma\varepsilon} \gamma V_t^{\varepsilon, \gamma} m(d\gamma) \right) dt + K^\varepsilon b(V_t^\varepsilon) dt + K^\varepsilon \sigma(V_t^\varepsilon) dB_t, \\ dV_t^{\varepsilon, \gamma} = (-\gamma V_t^{\varepsilon, \gamma} + b(V_t^\varepsilon)) dt + \sigma(V_t^\varepsilon) dB_t, \end{cases} \quad (8)$$

where the dynamics of the auxiliary process $X_t^\varepsilon := g(S_t^\varepsilon) - \rho f(v_t^\varepsilon)$ and the standard Brownian motion $B_t^\perp := \frac{W_t - \rho B_t}{\sqrt{1-\rho^2}}$ is independent from B_t with a constant correlation $\rho \in (-1, 1)$. Here

$$\begin{aligned} \theta(X_t^\varepsilon, V_t^\varepsilon) &:= \frac{\mu(S_t^\varepsilon, V_t^\varepsilon)}{\nu(S_t^\varepsilon)} - \frac{\nu'(S_t^\varepsilon)}{2} \varphi^2(V_t^\varepsilon) - \frac{\rho}{2} K^\varepsilon (\sigma(V_t^\varepsilon) \varphi'(V_t^\varepsilon) - \sigma'(V_t^\varepsilon) \varphi(V_t^\varepsilon)) \\ &\quad - \rho \left(- \int_0^\infty e^{-\gamma \varepsilon} \gamma V_t^{\varepsilon, \gamma} m(d\gamma) + K^\varepsilon b(V_t^\varepsilon) \right) \frac{\varphi(V_t^\varepsilon)}{K^\varepsilon \sigma(V_t^\varepsilon)}. \end{aligned} \quad (9)$$

Proof This proof follows similarly from Lemma 1 in [Cui et al. \(2018\)](#). \square

3.1 The construction of the CTMC approximation

We first recall the basic setup of CTMC. Denote

$$\begin{aligned} \mathcal{M} &:= \{1, 2, \dots, M\}, & \mathcal{M}^\circ &:= \{2, \dots, M-1\}, \\ \mathcal{N} &:= \{1, 2, \dots, N\}, & \mathcal{N}^\circ &:= \{2, \dots, N-1\}. \end{aligned}$$

Recall that a stochastic process $\alpha(t)$ taking values in the set \mathcal{M} of M possible states is a CTMC if the distribution of $\alpha(t + \Delta t)$, conditioned on the current state and the past history up to time t , depends only on the current state $\alpha(t)$. The transition dynamics of $\alpha(t)$ are characterized by the rate matrix $\mathbf{Q} = (q_{ij})_{M \times M}$, whose elements q_{ij} satisfy (i) $q_{ii} \leq 0$, and $q_{ij} \geq 0$, if $i \neq j$, and (ii) $\sum_j q_{ij} = 0$, $\forall i \in \mathcal{M}$.

In terms of q_{ij} , for a time increment $\Delta t \geq 0$, the transition probability matrix $\mathbf{P}(\Delta t)$ has the following matrix exponential representation:

$$\mathbf{P}(\Delta t) = \exp(\mathbf{Q} \cdot \Delta t) := \sum_{k=0}^{\infty} \frac{(\mathbf{Q} \cdot \Delta t)^k}{k!},$$

with elements $p_{ij}(\Delta t) := \text{Prob} \{ \alpha(t + \Delta t) = j \mid \alpha(t) = i \}$.

We first derive the CTMC approximation $\tilde{V}_t^\varepsilon \in \{v_1^\varepsilon, v_2^\varepsilon, \dots, v_M^\varepsilon\}$ of the variance process V_t^ε over a general non-uniform grid $\{v_i^\varepsilon\}_{i=1}^M$ for $i \in \mathcal{M}$. Recall (5) and let

$$\tilde{V}_t^\varepsilon = \tilde{V}_0^\varepsilon + \int_0^\infty e^{-\gamma \varepsilon} \tilde{V}_t^{\varepsilon, \gamma} m(d\gamma),$$

where $\tilde{V}_0^\varepsilon := V_0^\varepsilon$, $\tilde{V}_t^{\varepsilon, \gamma} \in \{v_i^{\varepsilon, \gamma}\}_{i=1}^M$ with $v_i^{\varepsilon, \gamma} = \frac{v_i^\varepsilon - V_0^\varepsilon}{\int_0^\infty e^{-\gamma \varepsilon} e^{-\gamma} m(d\gamma)} e^{-\gamma} =: \frac{v_i^\varepsilon - V_0^\varepsilon}{R} e^{-\gamma}$ and

$$\text{Prob} \left\{ \tilde{V}_t^{\varepsilon, \gamma} = v_i^{\varepsilon, \gamma} \mid \tilde{V}_t^\varepsilon = v_i^\varepsilon \right\} = 1.$$

Remark 3.1 *The relationship between $V_t^{\varepsilon, \gamma}$ and V_t^ε is given by the equation (5). Note that the solution of the integral equation (5) exists and is unique (see [Abi Jaber and El Euch \(2019c\)](#)). Thus there is a one-to-one correspondence between V_t^ε and $V_t^{\varepsilon, \gamma}$. Recall that V_t^ε is Markov, hence we can use a CTMC to approximate it, and the corresponding finite state space is v_i^ε . Note that the intermediate auxiliary process $V_t^{\varepsilon, \gamma}$ is not Markov, and we are not constructing a CTMC approximation to it. Hence $v_i^{\varepsilon, \gamma}$ should not be interpreted as the grid corresponding to a CTMC, but it is rather solved from the integral equation (5) when a value v_i^ε is substituted into that equation. Moreover, the variable γ in $V_t^{\varepsilon, \gamma}$ (defined by (6)) appears in the exponential form, which is the reason why $v_i^{\varepsilon, \gamma}$ is set to the*

form $\frac{v_i^\varepsilon - V_0^\varepsilon}{R} e^{-\gamma}$. As a by-product, for a given grid of the CTMC approximating V_t^ε , we have a uniquely defined corresponding value for $V_t^{\varepsilon,\gamma}$. Knowing this one-to-one link between a realization of the Markov process V_t^ε and the non-Markovian process $V_t^{\varepsilon,\gamma}$ is important, and is crucial for the design of the CTMC approximation to V_t^ε . Recall from (7) that the drift term of V_t^ε contains an integral with respect to $V_t^{\varepsilon,\gamma}$. Based on the above link, when we carry out moment matching to construct the CTMC approximation to V_t^ε , we can actually express the drift term as an explicit function of v_i^ε and separate the integral with respect to γ into a separate constant term R . This is the key advantage of the CTMC method as we avoid the discretization of the integral with respect to γ through a quadrature method, and this fact precisely leads to a dimension reduction. Essentially, the process $V_t^{\varepsilon,\gamma}$ is just an intermediate auxiliary process that is uniquely characterized through the integral equation (5). It does not need to be Markov, and the property of this intermediate process does not affect our construction of the CTMC approximation. We construct the CTMC approximation only to the X_t^ε and V_t^ε , but not $V_t^{\varepsilon,\gamma}$. To sum up, we use a CTMC \tilde{V}_t^ε to approximate V_t^ε based on its Markov property. We first establish the grid points v_i^ε , and then use the integral equation (5) to solve $v_i^{\varepsilon,\gamma}$ in terms of v_i^ε , and finally substitute it into the drift term of the SDE (7) of V_t^ε and set up moment matching equations to obtain the generator matrix of \tilde{V}_t^ε .

According to Mijatović and Pistorius (2013) and the SDE of V_t^ε in (7), the elements of the tridiagonal generator matrix $\mathbf{Q} = (q_{ij})_{M \times M}$ of \tilde{V}_t^ε for $i \in \mathcal{M}^\circ$, $j \in \mathcal{M}$, are uniquely determined through the following system of equations:

$$\begin{bmatrix} 1 & 1 & 1 \\ -h_i & 0 & h_{i+1} \\ h_i^2 & 0 & h_{i+1}^2 \end{bmatrix} \begin{bmatrix} q_{i,i-1} \\ q_{i,i} \\ q_{i,i+1} \end{bmatrix} = \begin{bmatrix} 0 \\ (v_i^\varepsilon - V_0^\varepsilon)\widehat{R} + K^\varepsilon b(v_i^\varepsilon) \\ (K^\varepsilon)^2 \sigma^2(v_i^\varepsilon) \end{bmatrix}, \quad (10)$$

where $h_i = v_i^\varepsilon - v_{i-1}^\varepsilon$, $\widehat{R} := -\int_0^\infty e^{-\gamma\varepsilon} \gamma e^{-\gamma} m(d\gamma)/R$, $q_{1,j} = q_{M,j} = 0$, $q_{i,j} = 0$ for $|i-j| > 1$, $i, j \in \mathcal{M}$. Solving (10) gives

$$\begin{cases} q_{i,i-1} = \frac{(K^\varepsilon)^2 \sigma^2(v_i^\varepsilon) - ((v_i^\varepsilon - V_0^\varepsilon)\widehat{R} + K^\varepsilon b(v_i^\varepsilon))h_{i+1}}{h_i(h_{i+1} + h_i)}, \\ q_{i,i} = \frac{-(K^\varepsilon)^2 \sigma^2(v_i^\varepsilon) + ((v_i^\varepsilon - V_0^\varepsilon)\widehat{R} + K^\varepsilon b(v_i^\varepsilon))(h_{i+1} - h_i)}{h_{i+1}h_i}, \\ q_{i,i+1} = \frac{(K^\varepsilon)^2 \sigma^2(v_i^\varepsilon) + ((v_i^\varepsilon - V_0^\varepsilon)\widehat{R} + K^\varepsilon b(v_i^\varepsilon))h_i}{h_{i+1}(h_{i+1} + h_i)}. \end{cases} \quad (11)$$

Thus the Markov process V_t^ε from (8) is approximated by a continuous-time Markov chain \tilde{V}_t^ε with the generator matrix $\mathbf{Q} = (q_{i,j})_{M \times M}$, whose entries are given in (11).

Remark 3.2 It is worth noting that the generator matrix $\mathbf{Q} = (q_{i,j})_{M \times M}$ of \tilde{V}_t^ε is well-defined and time-homogeneous. Each element $q_{i,j}$ shown in (11) is explicitly expressed, where v_i^ε and h_i are provided by grids design, R and \widehat{R} are both constants, and $K^\varepsilon = \varepsilon^{H-\frac{1}{2}}/\Gamma(H+1/2)$. Therefore, the CTMC method is fully explicit and very computational friendly.

Next, we derive the CTMC approximation $\tilde{X}_t^\varepsilon \in \{x_1^\varepsilon, x_2^\varepsilon, \dots, x_N^\varepsilon\}$ of the auxiliary process X_t^ε over a general non-uniform grid $\{x_i^\varepsilon\}_{i=1}^N$, where $x_i^\varepsilon = \sum_{\ell=1}^i \delta_\ell$ for $i \in \mathcal{N}$, and δ_ℓ is the grid interval. After approximating the variance process V_t^ε by the CTMC \tilde{V}_t^ε , the auxiliary process becomes a nonlinear regime-switching diffusion and its parameters have M states. In this way, we can use the technique introduced in Cui et al. (2018) to approximate X_t^ε by

a continuous-time Markov chain \tilde{X}_t^ε . In particular, according to (8), for each $\ell \in \mathcal{M}$, we define a second-layer Markov chain approximation which is determined by the rate matrix $\mathbf{\Lambda}_\ell = (\lambda_{ij}^\ell)_{N \times N}$ with

$$\begin{bmatrix} 1 & 1 & 1 \\ -\delta_i & 0 & \delta_{i+1} \\ \delta_i^2 & 0 & \delta_{i+1}^2 \end{bmatrix} \begin{bmatrix} \lambda_{i,i-1}^\ell \\ \lambda_{i,i}^\ell \\ \lambda_{i,i+1}^\ell \end{bmatrix} = \begin{bmatrix} 0 \\ \theta(x_i^\varepsilon, v_i^\varepsilon) \\ (1-\rho^2)\varphi^2(v_i^\varepsilon) \end{bmatrix}, \quad (12)$$

where $\lambda_{1i}^\ell = \lambda_{Ni}^\ell = 0$ and $\lambda_{i,j}^\ell = 0$ for $|i-j| > 1$, $i, j \in \mathcal{N}$ and $\ell \in \mathcal{M}$. Solving (12) gives

$$\begin{cases} \lambda_{i,i-1}^\ell = \frac{(1-\rho^2)\varphi^2(v_i^\varepsilon) - \theta(x_i^\varepsilon, v_i^\varepsilon)\delta_{i+1}}{\delta_i(\delta_{i+1} + \delta_i)}, \\ \lambda_{i,i}^\ell = \frac{-(1-\rho^2)\varphi^2(v_i^\varepsilon) + \theta(x_i^\varepsilon, v_i^\varepsilon)(\delta_{i+1} - \delta_i)}{\delta_{i+1}\delta_i}, \\ \lambda_{i,i+1}^\ell = \frac{(1-\rho^2)\varphi^2(v_i^\varepsilon) + \theta(x_i^\varepsilon, v_i^\varepsilon)\delta_i}{\delta_{i+1}(\delta_{i+1} + \delta_i)}. \end{cases} \quad (13)$$

Note that $\lambda_{i,j}^\ell$ is well-defined for $i, j \in \mathcal{N}$, $\ell \in \mathcal{M}$, where

$$\begin{aligned} \theta(x_i^\varepsilon, v_i^\varepsilon) &= \frac{\mu(s_{i,\ell}^\varepsilon, v_i^\varepsilon)}{\nu(s_{i,\ell}^\varepsilon)} - \frac{\nu'(s_{i,\ell}^\varepsilon)}{2}\varphi^2(v_i^\varepsilon) + \frac{\rho}{2}(\sigma(v_i^\varepsilon)\varphi'(v_i^\varepsilon) - \sigma'(v_i^\varepsilon)\varphi(v_i^\varepsilon)) \\ &\quad - \rho \left((v_i^\varepsilon - V_0^\varepsilon)\widehat{R} + \frac{\varepsilon^{H-\frac{1}{2}}b(v_i^\varepsilon)}{\Gamma(H+1/2)} \right) \frac{\varphi(v_i^\varepsilon)\Gamma(H+1/2)}{\varepsilon^{H-\frac{1}{2}}\sigma(v_i^\varepsilon)}, \end{aligned}$$

with $s_{i,\ell}^\varepsilon = g^{-1}(x_i^\varepsilon + \rho f(v_i^\varepsilon))$.

According to Song et al. (2016), $(\tilde{X}_t^\varepsilon, \tilde{V}_t^\varepsilon)$ can be represented as a one-dimensional CTMC with a $NM \times NM$ transition rate matrix:

$$\mathbf{\Lambda} = \begin{pmatrix} q_{11}\mathbf{I}_N + \mathbf{\Lambda}_1 & q_{12}\mathbf{I}_N & \cdots & q_{1M}\mathbf{I}_N \\ q_{21}\mathbf{I}_N & q_{22}\mathbf{I}_N + \mathbf{\Lambda}_2 & \cdots & q_{2M}\mathbf{I}_N \\ \vdots & \vdots & \ddots & \vdots \\ q_{M1}\mathbf{I}_N & q_{M2}\mathbf{I}_N & \cdots & q_{MM}\mathbf{I}_N + \mathbf{\Lambda}_M \end{pmatrix}, \quad (14)$$

where \mathbf{I}_N is the $N \times N$ identity matrix, $q_{i,j}$ and $\mathbf{\Lambda}_l = (\lambda_{i,j}^l)_{N \times N}$ are respectively given by (11) and (13). Recall (8) and denote

$$\tilde{S}_t^\varepsilon := g^{-1}(\tilde{X}_t^\varepsilon + \rho f(\tilde{V}_t^\varepsilon)).$$

Then for any continuous function ϕ , with the setting that $g(s^\varepsilon) - \rho f(v^\varepsilon) = x^\varepsilon = x_i^\varepsilon$, $v^\varepsilon = v_i^\varepsilon$,

$$\begin{aligned} &\mathbb{E}[\phi(S_T^\varepsilon, V_T^\varepsilon) | S_t^\varepsilon = s^\varepsilon, V_t^\varepsilon = v^\varepsilon] \\ &= \mathbb{E}[\phi(g^{-1}(X_t^\varepsilon + \rho f(V_t^\varepsilon)), V_T^\varepsilon) | X_t^\varepsilon = x^\varepsilon, V_t^\varepsilon = v^\varepsilon] \\ &\approx \mathbb{E}[\phi(g^{-1}(\tilde{X}_t^\varepsilon + \rho f(\tilde{V}_t^\varepsilon)), \tilde{V}_T^\varepsilon) | \tilde{X}_t^\varepsilon = x_i^\varepsilon, \tilde{V}_t^\varepsilon = v_i^\varepsilon] \\ &= \mathbf{e}_{i,l} \cdot \exp(\mathbf{\Lambda}(T-t)) \cdot \mathbf{\Phi}, \end{aligned} \quad (15)$$

where $\mathbf{e}_{i,l}$ is a $1 \times MN$ vector with all entries equal to 0 except that the $(l-1)N+i$ entry is equal to 1, $\mathbf{\Lambda}$ is given by (14), and the payoff vector $\mathbf{\Phi}$ an $MN \times 1$ vectors with elements $\mathbf{\Phi}_{(l-1)N+i} = \phi(g^{-1}(x_i^\varepsilon + \rho f(v_i^\varepsilon)), v_i^\varepsilon)$, for $l \in \mathcal{M}$, $i \in \mathcal{N}$.

3.2 Convergence analysis for the CTMC approximation

Denote $\mathbb{S} := [s_{\min}, s_{\max}]$ for $-\infty < s_{\min} < s_{\max} < \infty$. Let $\mathbb{S}^\varepsilon := [s_{\min}^\varepsilon, s_{\max}^\varepsilon]$, $\mathbb{V}^\varepsilon := [v_{\min}^\varepsilon, v_{\max}^\varepsilon]$, $\mathbb{X}^\varepsilon := [x_{\min}^\varepsilon, x_{\max}^\varepsilon]$ and $\mathbb{T} := [0, T]$ be the range of the asset process S_t^ε , volatility process V_t^ε , auxiliary process X_t^ε and time t , where $-\infty < s_{\min}^\varepsilon < s_{\max}^\varepsilon < \infty$, $-\infty < v_{\min}^\varepsilon < v_{\max}^\varepsilon < \infty$, $x_{\min}^\varepsilon = g(s_{\min}^\varepsilon) + \rho f(v_{\min}^\varepsilon)$ and $x_{\max}^\varepsilon = g(s_{\max}^\varepsilon) + \rho f(v_{\max}^\varepsilon)$. The convergence analysis of the CTMC approximation is based on the following lemma.

Lemma 3.1 *Let $S_t \in \mathbb{S}$ for $t \in \mathbb{T}$ be a Feller process whose infinitesimal generator is given by*

$$\mathcal{L}G(s) := \lim_{t \rightarrow 0} \frac{\mathbb{E}[G(S_t)|S_0 = s] - G(s)}{t}.$$

Let $\tilde{S}_t^n \in \mathbb{S}^n$ be the continuous-time Markov chain with the generator \mathcal{L}^n , $\mathbb{S}^n \subseteq \mathbb{S}$ and when n tends to infinity, $\mathbb{S}^n = \mathbb{S}$. Assume that for each $G \in \mathcal{C}^2(\mathbb{S})$,

$$\lim_{n \rightarrow \infty} \max_{s \in \mathbb{S}^n} |\mathcal{L}G(s) - \mathcal{L}^n G(s)| = 0. \quad (16)$$

Then \tilde{S}_t^n converges weakly to S_t as n goes to infinity.

Proof According to Section 8.7 in [Durrett \(2018\)](#) and Theorem 10.1.1 in [Kushner and Dupuis \(2001\)](#), it can be deduced from condition (16) that \tilde{S}_t^n is tight. Then by Theorem 4.2.11 in [Ethier \(2009\)](#), we obtain the weak convergence of \tilde{S}_t^n to S_t . This completes the proof. \square

The first theorem gives the weak convergence of \tilde{V}_t^ε to V_t^ε .

Theorem 3.1 *Assuming that the grid interval h satisfies: $h_\ell = \mathcal{O}(M^{-1})$, $|h_\ell - h_{\ell+1}| \leq \mathcal{O}(M^{-2})$ and Assumption 2.1 holds, the continuous-time Markov chain \tilde{V}_t^ε with the generator $\mathbf{Q} = (q_{i,j})_{M \times M}$ converges weakly to V_t^ε , as M goes to infinity.*

Proof Theorem 2.4 shows the Markov property of V_t^ε . According to the continuity of Riemann integral, V_t^ε in (3) has continuous simple path, therefore is a Feller process. Here we assume that $\text{Prob}\{V_t^{\varepsilon,\gamma} = v_\ell^\varepsilon | V_t^\varepsilon = v_\ell^\varepsilon\} = 1$. Moreover, for $G \in \mathcal{C}^2(\mathbb{V}^\varepsilon)$, $\ell \in \mathcal{M}^\circ$,

$$\begin{aligned} |\mathcal{L}G(v_\ell^\varepsilon) - \mathbf{Q}G(v_\ell^\varepsilon)| &= \left| \frac{1}{2}(K^\varepsilon)^2 \sigma^2(v_\ell^\varepsilon) G''(v_\ell^\varepsilon) + \left((v_\ell^\varepsilon - V_0^\varepsilon) \hat{R} + K^\varepsilon b(v_\ell^\varepsilon) \right) G'(v_\ell^\varepsilon) \right. \\ &\quad \left. - (q_{\ell, \ell-1} G(v_{\ell-1}^\varepsilon) + q_{\ell, \ell} G(v_\ell^\varepsilon) + q_{\ell, \ell+1} G(v_{\ell+1}^\varepsilon)) \right|. \end{aligned}$$

Then we use (11), the triangle inequality, the Lipschitz continuity and the linear growth of b and σ to give

$$\begin{aligned} &|\mathcal{L}G(v_\ell^\varepsilon) - \mathbf{Q}G(v_\ell^\varepsilon)| \\ &\leq C \left[\left| G''(v_\ell^\varepsilon) - \frac{2}{(h_{\ell+1} + h_\ell)} \left(\frac{G(v_{\ell+1}^\varepsilon) - G(v_\ell^\varepsilon)}{h_{\ell+1}} - \frac{G(v_\ell^\varepsilon) - G(v_{\ell-1}^\varepsilon)}{h_\ell} \right) \right| \right. \\ &\quad \left. + \left| G'(v_\ell^\varepsilon) - \frac{1}{(h_{\ell+1} + h_\ell)} \left(h_\ell (G(v_{\ell+1}^\varepsilon) - G(v_\ell^\varepsilon)) + \frac{h_{\ell+1} (G(v_\ell^\varepsilon) - G(v_{\ell-1}^\varepsilon))}{h_\ell} \right) \right| \right]. \end{aligned} \quad (17)$$

By Taylor expansion, we have that

$$\begin{aligned} G(v_{\ell+1}^\varepsilon) &= G(v_\ell^\varepsilon) + G'(v_\ell^\varepsilon) h_{\ell+1} + G''(v_\ell^\varepsilon) \frac{h_{\ell+1}^2}{2} + o(h_{\ell+1}^2), \\ G(v_{\ell-1}^\varepsilon) &= G(v_\ell^\varepsilon) - G'(v_\ell^\varepsilon) h_\ell + G''(v_\ell^\varepsilon) \frac{h_\ell^2}{2} + o(h_\ell^2). \end{aligned} \quad (18)$$

Plugging (18) into (17) and using the condition $h_\ell = \mathcal{O}(M^{-1})$, $|h_\ell - h_{\ell+1}| \leq \mathcal{O}(M^{-2})$, we obtain

$$|\mathcal{L}G(v_\ell^\varepsilon) - \mathbf{Q}^\gamma G(v_\ell^\varepsilon)| \leq o(1).$$

Then by Lemma 3.1, \tilde{V}_t^ε converges weakly to V_t^ε as M goes to infinity. This completes the proof. \square

The next theorem shows the weak convergence of \tilde{X}_t^ε to X_t^ε .

Theorem 3.2 *Assuming that Assumption 2.1 holds, the grid interval h , δ satisfy: $h_\ell = \mathcal{O}(M^{-1})$, $|h_\ell - h_{\ell+1}| \leq \mathcal{O}(M^{-2})$, and $\delta_i = \mathcal{O}(N^{-1})$, $|\delta_i - \delta_{i+1}| \leq \mathcal{O}(N^{-2})$, the continuous-time Markov chain \tilde{X}_t^ε converges weakly to X_t^ε , as M, N go to infinity.*

Proof It is easy to verify that under Assumption 2.1, $\theta(x^\varepsilon, v^\varepsilon)$, which is the drift term of X_t^ε and defined by (9), is continuous and bounded for $(x^\varepsilon, v^\varepsilon) \in \mathbb{X}^\varepsilon \times \mathbb{V}^\varepsilon$. Then by similar arguments as Theorem 3.1, we can obtain the desired conclusion. This completes the proof. \square

4 Option pricing under RSLV model

In this section, we use the semimartingale and CTMC approximation techniques to give the explicit approximate expression of option prices under the RSLV model.

Vanilla option prices for (S_T, V_T) under the RSLV model (1) is given by:

$$\mathbb{E} [e^{-rT} \phi(S_T, V_T) | S_0 = s, V_0 = v],$$

where

$$\phi(S_T, V_T) = \begin{cases} (S_T - D)^+ & \text{for a call,} \\ (D - S_T)^+ & \text{for a put,} \end{cases}$$

and r is the risk-free interest rate, D is the strike price, and T is the maturity. After the semimartingale approximation of (S_T, V_T) by $(S_T^\varepsilon, V_T^\varepsilon)$, and the CTMC approximation by $(\tilde{S}_T^\varepsilon, \tilde{V}_T^\varepsilon)$, the European options prices under the RSLV model have the following approximate formula.

Algorithm 4.1 (European options) *Given that $s = s^\varepsilon$, $v = v^\varepsilon = v_i^\varepsilon$ and $x_i^\varepsilon = g(s^\varepsilon) + \rho f(v_i^\varepsilon)$, the European option price under the RSLV model can be approximately calculated by*

$$\begin{aligned} & \mathbb{E} [e^{-rT} \phi(S_T, V_T) | S_0 = s, V_0 = v] \\ & \approx \mathbb{E} [e^{-rT} \phi(S_T^\varepsilon, V_T^\varepsilon) | S_0^\varepsilon = s^\varepsilon, V_0^\varepsilon = v^\varepsilon] \\ & \approx \mathbb{E} [e^{-rT} \phi(g^{-1}(\tilde{X}_T^\varepsilon + \rho f(\tilde{V}_T^\varepsilon)), \tilde{V}_T^\varepsilon) | \tilde{X}_0^\varepsilon = x_i^\varepsilon, \tilde{V}_0^\varepsilon = v_i^\varepsilon] \\ & = e^{-rT} \cdot \mathbf{e}_{i,l} \cdot \exp(\mathbf{\Lambda}T) \cdot \mathbf{\Phi}^{(1)}. \end{aligned}$$

Here $\mathbf{e}_{i,l}$ is a $1 \times NM$ vector with all entries equal to 0 except that the $(l-1)N + i$ entry is equal to 1, $\mathbf{\Lambda}$ is given by (14), and $\mathbf{\Phi}^{(1)}$ is an $NM \times 1$ vector with elements for $l \in \mathcal{M}$, $i \in \mathcal{N}$,

$$\mathbf{\Phi}^{(1)}_{(l-1)N+i} = \phi(g^{-1}(x_i^\varepsilon + \rho f(v_l^\varepsilon))) = \begin{cases} (g^{-1}(x_i^\varepsilon + \rho f(v_l^\varepsilon)) - D)^+ & \text{for a call,} \\ (D - g^{-1}(x_i^\varepsilon + \rho f(v_l^\varepsilon)))^+ & \text{for a put.} \end{cases}$$

Similarly, we have the semimartingale and CTMC approximate formula of barrier options prices under the RSLV model.

Algorithm 4.2 (barrier options) *Given that $s = s^\varepsilon$, $v = v^\varepsilon = v_l^\varepsilon$ and $x_i^\varepsilon = g(s^\varepsilon) + \rho f(v_l^\varepsilon)$, the barrier option price under the RSLV model with $0 \leq L < U < \infty$, can be approximately calculated by*

$$\begin{aligned} & \mathbb{E} \left[e^{-rT} \phi(S_T, V_T) \mathbf{1}_{\{L < S_T < U\}} | S_0 = s, V_0 = v \right] \\ & \approx \mathbb{E} \left[e^{-rT} \phi(S_T^\varepsilon, V_T^\varepsilon) \mathbf{1}_{\{L < S_T < U\}} | S_0^\varepsilon = s^\varepsilon, V_0^\varepsilon = v^\varepsilon \right] \\ & \approx \mathbb{E} \left[e^{-rT} \phi(g^{-1}(\tilde{X}_T^\varepsilon + \rho f(\tilde{V}_T^\varepsilon)), \tilde{V}_T^\varepsilon) \mathbf{1}_{\{L < g^{-1}(\tilde{X}_T^\varepsilon + \rho f(\tilde{V}_T^\varepsilon)) < U\}} | \tilde{X}_0^\varepsilon = x_i^\varepsilon, \tilde{V}_0^\varepsilon = v_l^\varepsilon \right] \\ & = e^{-rT} \cdot \mathbf{e}_{i,l} \cdot \exp(\mathbf{\Lambda}T) \cdot \mathbf{\Phi}^{(2)}. \end{aligned}$$

Here $\mathbf{e}_{i,l}$ is a $1 \times NM$ vector with all entries equal to 0 except that the $(l-1)N + i$ entry is equal to 1, $\mathbf{\Lambda}$ is given by (14), and $\mathbf{\Phi}^{(2)}$ is an $NM \times 1$ vector with elements for $l \in \mathcal{M}$, $i \in \mathcal{N}$,

$$\mathbf{\Phi}^{(2)}_{(l-1)N+i} = \begin{cases} (g^{-1}(x_i^\varepsilon + \rho f(v_l^\varepsilon)) - D)^+ \mathbf{1}_{\{L < g^{-1}(x_i^\varepsilon + \rho f(v_l^\varepsilon)) < U\}} & \text{for a call,} \\ (D - g^{-1}(x_i^\varepsilon + \rho f(v_l^\varepsilon)))^+ \mathbf{1}_{\{L < g^{-1}(x_i^\varepsilon + \rho f(v_l^\varepsilon)) < U\}} & \text{for a put.} \end{cases}$$

Next we consider (finite-maturity) American options, whose prices are given by

$$\max_{\tau \in \mathcal{T}} \mathbb{E} \left[e^{-r\tau} \phi(S_\tau, V_\tau) | S_0 = s, V_0 = v \right],$$

where the set \mathcal{T} comprises of the collection of \mathbb{F} -stopping times taking values between 0 and T . This means that American options can be exercised at any time in $[0, T]$. \mathcal{T} can be approximated by a finite set of admissible exercise times $\mathcal{T}^n := \{\tau_i\}_{i=0}^n$, where $\tau_i = \frac{iT}{n}$, where n is the number of monitoring dates. Under admissible exercise times set \mathcal{T}^n , the option is called the Bermudan option. By semimartingale and CTMC approximations, the value of the American option under the RSLV model can be approximately expressed as:

Algorithm 4.3 (American options) *Given that $s = s^\varepsilon$, $v = v^\varepsilon = v_l^\varepsilon$ and $x_i^\varepsilon = g(s^\varepsilon) + \rho f(v_l^\varepsilon)$, the Bermudan option price under RSLV model can be approximately calculated by*

$$\begin{aligned} & \max_{\tau \in \mathcal{T}} \mathbb{E} \left[e^{-r\tau} \phi(S_\tau, V_\tau) | S_0 = s, V_0 = v \right] \\ & \approx \max_{\tau \in \mathcal{T}^n} \mathbb{E} \left[e^{-r\tau} \phi(S_\tau, V_\tau) | S_0 = s, V_0 = v \right] \\ & \approx \max_{\tau \in \mathcal{T}^n} \mathbb{E} \left[e^{-r\tau} \phi(S_\tau^\varepsilon, V_\tau^\varepsilon) | S_0^\varepsilon = s^\varepsilon, V_0^\varepsilon = v^\varepsilon \right] \\ & \approx \max_{\tau \in \mathcal{T}^n} \mathbb{E} \left[e^{-r\tau} \phi(g^{-1}(\tilde{X}_\tau^\varepsilon + \rho f(\tilde{V}_\tau^\varepsilon)), \tilde{V}_\tau^\varepsilon) | \tilde{X}_0^\varepsilon = x_i^\varepsilon, \tilde{V}_0^\varepsilon = v_l^\varepsilon \right] =: B_0, \end{aligned}$$

where $B_0 = \mathbf{e}_{i,l} \cdot \mathbf{B}_0$, and

$$\begin{cases} \mathbf{B}_n = \mathbf{\Phi}^{(1)}, \\ \mathbf{B}_i = \max \left\{ e^{-rT/n} \exp(\mathbf{\Lambda}T/n) \cdot \mathbf{B}_{i+1}, \mathbf{\Phi}^{(1)} \right\}, \quad i = n-1, n-2, \dots, 0. \end{cases}$$

Here \mathbf{B}_i is a $NM \times 1$ vector, $\mathbf{e}_{i,l}$ a $1 \times NM$ vector with all entries equal to 0 except that the $(l-1)N+i$ entry is equal to 1, $\mathbf{\Lambda}$ is given by (14), and $\Phi^{(1)}$ is an $NM \times 1$ vector with elements for $l \in \mathcal{M}$, $i \in \mathcal{N}$,

$$\Phi^{(1)}_{(l-1)N+i} = \phi(g^{-1}(x_i^\varepsilon + \rho f(v_l^\varepsilon))) = \begin{cases} (g^{-1}(x_i^\varepsilon + \rho f(v_l^\varepsilon)) - D)^+ & \text{for a call,} \\ (D - g^{-1}(x_i^\varepsilon + \rho f(v_l^\varepsilon)))^+ & \text{for a put.} \end{cases}$$

Remark 4.1 (Convergence analysis of options pricing) Note that Theorem 2.2 and Theorem 3.2 show respectively the weak convergence of the semimartingale approximation and the CTMC approximation. For European and barrier options, since the functions ϕ , g , f are all continuous, the options prices obtained by the semimartingale and CTMC approximations converge to the original RSLV options prices, due to the continuous mapping theorem (see, e.g., Kushner and Dupuis (2001)). For American options, the weak convergence follows from the following three types of convergence: the convergence of time step discretization (refer to Chapter 2.4 in Quecke (2007)), semimartingale approximation (due to continuous mapping theorem), and the CTMC approximation (see Section 6 in Eriksson and Pistorius (2015)).

5 Numerical results

In this section, we extend the traditional stochastic local volatility model (see Table 1) to rough stochastic local volatility model (see Table 2). Then a series of examples for European, barrier and American options are used to illustrate the accuracy and efficiency of the semimartingale and CTMC approximation method introduced in Section 4. All numerical experiments are carried out with Matlab R2016a on a Core i7 desktop with 16GB RAM and speed 3.60 GHz.

Table 1 collects some popular stochastic local volatility models in the literature. The traditional stochastic local volatility models are all driven by standard Brownian motions. However, as confirmed by Gatheral et al. (2018), for a very wide range of assets, historical fluctuation time series exhibit rougher behavior than the Brownian motion. Therefore, it is very practical to recast the traditional stochastic local volatility models in the rough setting. Similar to the way El Euch and Rosenbaum (2019) deducing the rough Heston model, we generalize all models listed in Table 1 to their rough counterparts. The results are listed in Table 2. In order to numerically solve the option pricing problem under RSLV models, we use the semimartingale approximation introduced in Section 2.2 and auxiliary processes introduced in Lemma 3.1 to approximately transform those models into PSLV models with two independent Brownian motions. The results are listed in Table 3.

Next, we use the method introduced in Section 4 to numerically solve the European and barrier options pricing under RSLV models. All models considered in this paper share the same set of parameters:

$$\begin{aligned} S_0 = 10, V_0 = 0.04, T = 1, D = 4, \rho = -0.75, r = 0, \sigma = 0.8, \beta = 0.7, \\ \eta = 4, \vartheta = 0.035, a = 0.02, b = 0.05, c = 1, L = 2, U = 15, H = 0.12. \end{aligned}$$

In the numerical implementation, we use the same boundary points $v_{\min} = 10^{-3}V_0$, $v_{\max} = 4V_0$, $s_{\min} = 10^{-3}S_0$, $s_{\max} = 4S_0$ and $x_{\min} = 10^{-3}X_0$, $x_{\max} = 4X_0$, with $X_0 = g(S_0) - \rho f(v_0)$ and choose the piecewise uniform grids.

Table 1: Examples of the stochastic local volatility models.

Heston (Heston (1993))	$dS_t = (r - q)S_t dt + S_t \sqrt{V_t} dW_t$ $dV_t = \eta(\vartheta - V_t) dt + \sigma \sqrt{V_t} dB_t$	$\eta, \vartheta \in \mathbb{R}$ $\sigma > 0$
4/2 model (Grasselli (2017))	$dS_t = (r - q)S_t dt + S_t [a\sqrt{V_t} + b/\sqrt{V_t}] dW_t$ $dV_t = \eta(\vartheta - V_t) dt + \sigma \sqrt{V_t} dB_t$	$\eta, \vartheta, a, b \in \mathbb{R}$ $\sigma > 0$
α -Hyper (Da Fonseca and Martini (2016))	$dS_t = (r - q)S_t dt + S_t \exp(V_t) dW_t$ $dV_t = (\eta - \vartheta \exp(aV_t)) dt + \sigma dB_t$	$\eta \in \mathbb{R}$ $\vartheta, a, \sigma > 0$
SABR (Hagan et al. (2002))	$dS_t = V_t S_t^\beta dW_t$ $dV_t = \sigma V_t dB_t$	$\beta \in [0, 1)$ $\sigma > 0$
Heston-SABR (Van der Stoep et al. (2014))	$dS_t = (r - q)S_t dt + \sqrt{V_t} S_t^\beta dW_t$ $dV_t = \eta(\vartheta - V_t) dt + \sigma \sqrt{V_t} dB_t$	$\beta \in [0, 1)$ $\eta, \vartheta, \sigma > 0$
Quadratic SLV (Lipton (2002))	$dS_t = (r - q)S_t dt + \sqrt{V_t}(aS_t^2 + bS_t + c) dW_t$ $dV_t = \eta(\vartheta - V_t) dt + \sigma \sqrt{V_t} dB_t$	$4ac > b^2$ $a, \eta, \vartheta, \sigma > 0$

* Here r is the risk-free interest rate, q is the dividend yield, V_t is the volatility and satisfies different stochastic differential equation for different models.

Table 2: Examples of the rough stochastic local volatility models.

Rough Heston	$dS_t = (r - q)S_t dt + S_t \sqrt{V_t} dW_t$ $V_t = V_0 + \int_0^t K(t, s) (\eta(\vartheta - V_s) ds + \sigma \sqrt{V_s} dB_s)$	$\eta, \vartheta \in \mathbb{R}$ $\sigma > 0$
Rough 4/2 model	$dS_t = (r - q)S_t dt + S_t [a\sqrt{V_t} + b/\sqrt{V_t}] dW_t$ $V_t = V_0 + \int_0^t K(t, s) (\eta(\vartheta - V_s) ds + \sigma \sqrt{V_s} dB_s)$	$\eta, \vartheta, a, b \in \mathbb{R}$ $\sigma > 0$
Rough α -Hyper	$dS_t = (r - q)S_t dt + S_t \exp(V_t) dW_t$ $V_t = V_0 + \int_0^t K(t, s) ((\eta - \vartheta \exp(aV_s)) ds + \sigma dB_s)$	$\eta \in \mathbb{R}$ $\vartheta, a, \sigma > 0$
Rough SABR	$dS_t = V_t S_t^\beta dW_t$ $V_t = V_0 + \int_0^t K(t, s) (\sigma V_s dB_s)$	$\beta \in [0, 1)$ $\sigma > 0$
Rough Heston-SABR	$dS_t = (r - q)S_t dt + \sqrt{V_t} S_t^\beta dW_t$ $V_t = V_0 + \int_0^t K(t, s) (\eta(\vartheta - V_s) ds + \sigma \sqrt{V_s} dB_s)$	$\beta \in [0, 1)$ $\eta, \vartheta, \sigma > 0$
Rough quadratic SLV	$dS_t = (r - q)S_t dt + \sqrt{V_t}(aS_t^2 + bS_t + c) dW_t$ $V_t = V_0 + \int_0^t K(t, s) (\eta(\vartheta - V_s) ds + \sigma \sqrt{V_s} dB_s)$	$4ac > b^2$ $a, \eta, \vartheta, \sigma > 0$

* Here r is the risk-free interest rate, q is the dividend yield, V_t is the volatility process with initial value $V_0 > 0$, and $K(t, s) = (t - s)^{H - \frac{1}{2}} / \Gamma(H + 1/2)$ is the fractional kernel with the Hurst parameter $H \in (0, 1/2)$.

Table 3: Examples of dynamics and variance transforms for the perturbed stochastic local volatility models.

Perturbed Heston	$\begin{cases} dX_t^\varepsilon = \left(r - q - \frac{V_t^\varepsilon}{2} - \frac{\rho\eta(\vartheta - V_t^\varepsilon)}{\sigma} + \frac{\rho\chi(V_t^{\varepsilon,\gamma})}{K^\varepsilon\sigma} \right) dt + \sqrt{1 - \rho^2} \sqrt{V_t^\varepsilon} dB_t^\perp \\ dV_t^\varepsilon = -\chi(V_t^{\varepsilon,\gamma}) dt + K^\varepsilon (\eta(\vartheta - V_t^\varepsilon) dt + \sigma \sqrt{V_t^\varepsilon} dB_t) \\ dV_t^{\varepsilon,\gamma} = (-\gamma V_t^{\varepsilon,\gamma} + \eta(\vartheta - V_t^\varepsilon)) dt + \sigma \sqrt{V_t^\varepsilon} dB_t \\ X_t^\varepsilon = \log S_t^\varepsilon - \frac{\rho V_t^\varepsilon}{K^\varepsilon\sigma} \end{cases}$
Perturbed 4/2 model	$\begin{cases} dX_t^\varepsilon = \left(r - q + \frac{\rho}{\sigma} \left(\frac{\chi(V_t^{\varepsilon,\gamma})}{K^\varepsilon} - \eta(\vartheta - V_t^\varepsilon) \right) \left(a + \frac{b}{V_t^\varepsilon} \right) - \frac{\rho K^\varepsilon b \sigma}{2V_t^\varepsilon} \right) dt \\ \quad - \frac{1}{2} \left(a \sqrt{V_t^\varepsilon} + \frac{b}{\sqrt{V_t^\varepsilon}} \right)^2 dt + \sqrt{1 - \rho^2} \left(a \sqrt{V_t^\varepsilon} + \frac{b}{\sqrt{V_t^\varepsilon}} \right) dB_t^\perp \\ dV_t^\varepsilon = -\chi(V_t^{\varepsilon,\gamma}) dt + K^\varepsilon (\eta(\vartheta - V_t^\varepsilon) dt + \sigma \sqrt{V_t^\varepsilon} dB_t) \\ dV_t^{\varepsilon,\gamma} = (-\gamma V_t^{\varepsilon,\gamma} + \eta(\vartheta - V_t^\varepsilon)) dt + \sigma \sqrt{V_t^\varepsilon} dB_t \\ X_t^\varepsilon = \log S_t^\varepsilon - \rho \frac{aV_t^\varepsilon + b \log V_t^\varepsilon}{K^\varepsilon\sigma} \end{cases}$
Perturbed α -Hyper	$\begin{cases} dX_t^\varepsilon = \left(r - q - \frac{\rho \exp(V_t^\varepsilon)}{\sigma} \left(\frac{\chi(V_t^{\varepsilon,\gamma})}{K^\varepsilon} - \eta + \vartheta \exp(aV_t^\varepsilon) \right) dt \right. \\ \quad \left. + \left(\frac{\rho K^\varepsilon \sigma \exp(V_t^\varepsilon)}{\sigma} - \frac{\exp(2V_t^\varepsilon)}{2} \right) dt + \sqrt{1 - \rho^2} \exp(V_t^\varepsilon) dB_t^\perp \right) \\ dV_t^\varepsilon = -\chi(V_t^{\varepsilon,\gamma}) dt + K^\varepsilon ((\eta - \vartheta \exp(aV_t^\varepsilon)) dt + \sigma dB_t) \\ dV_t^{\varepsilon,\gamma} = (-\gamma V_t^{\varepsilon,\gamma} + \eta - \vartheta \exp(aV_t^\varepsilon)) dt + \sigma dB_t \\ X_t^\varepsilon = \log S_t^\varepsilon - \frac{\rho \exp(V_t^\varepsilon)}{K^\varepsilon\sigma} \end{cases}$
Perturbed SABR	$\begin{cases} dX_t^\varepsilon = \left(-\frac{\beta v_t^2}{2(1-\beta) \left(X_t^\varepsilon + \frac{\rho V_t^\varepsilon}{K^\varepsilon\sigma} \right)} + \frac{\rho\chi(V_t^{\varepsilon,\gamma})}{K^\varepsilon\sigma} \right) dt + \sqrt{1 - \rho^2} V_t^\varepsilon dB_t^\perp \\ dV_t^\varepsilon = -\chi(V_t^{\varepsilon,\gamma}) dt + K^\varepsilon \sigma V_t^\varepsilon dB_t \\ dV_t^{\varepsilon,\gamma} = -\gamma V_t^{\varepsilon,\gamma} dt + \sigma V_t^\varepsilon dB_t \\ X_t^\varepsilon = \frac{(S_t^\varepsilon)^{1-\beta}}{1-\beta} - \frac{\rho V_t^\varepsilon}{K^\varepsilon\sigma} \end{cases}$
Perturbed Heston-SABR	$\begin{cases} dX_t^\varepsilon = \left((r - q)(1 - \beta) \left(X_t^\varepsilon + \frac{\rho V_t^\varepsilon}{K^\varepsilon\sigma} \right) - \frac{\beta V_t^\varepsilon}{2(1-\beta) \left(X_t^\varepsilon + \frac{\rho V_t^\varepsilon}{K^\varepsilon\sigma} \right)} \right) dt \\ \quad + \frac{\rho}{\sigma} \left(\frac{\chi(V_t^{\varepsilon,\gamma})}{K^\varepsilon} - \eta(\vartheta - V_t^\varepsilon) \right) dt + \sqrt{1 - \rho^2} \sqrt{v_t} dB_t^\perp \\ dV_t^\varepsilon = -\chi(V_t^{\varepsilon,\gamma}) dt + K^\varepsilon (\eta(\vartheta - V_t^\varepsilon) dt + \sigma \sqrt{V_t^\varepsilon} dB_t) \\ dV_t^{\varepsilon,\gamma} = (-\gamma V_t^{\varepsilon,\gamma} + \eta(\vartheta - V_t^\varepsilon)) dt + \sigma \sqrt{V_t^\varepsilon} dB_t \\ X_t^\varepsilon = \frac{(S_t^\varepsilon)^{1-\beta}}{1-\beta} - \frac{\rho V_t^\varepsilon}{K^\varepsilon\sigma} \end{cases}$
Perturbed quadratic SLV	$\begin{cases} dX_t^\varepsilon = \left(\frac{(r-q)S_t^\varepsilon}{a(S_t^\varepsilon)^2 + bS_t^\varepsilon + c} - \frac{2aS_t^\varepsilon + b}{2} V_t^\varepsilon + \frac{\rho}{\sigma} \left(\frac{\chi(V_t^{\varepsilon,\gamma})}{K^\varepsilon} - \eta(\vartheta - V_t^\varepsilon) \right) \right) dt \\ \quad + \sqrt{1 - \rho^2} \sqrt{v_t} dB_t^\perp \\ dV_t^\varepsilon = -\chi(V_t^{\varepsilon,\gamma}) dt + K^\varepsilon (\eta(\vartheta - V_t^\varepsilon) dt + \sigma \sqrt{V_t^\varepsilon} dB_t) \\ dV_t^{\varepsilon,\gamma} = (-\gamma V_t^{\varepsilon,\gamma} + \eta(\vartheta - V_t^\varepsilon)) dt + \sigma \sqrt{V_t^\varepsilon} dB_t \\ X_t^\varepsilon = \frac{2 \arctan \left(\frac{2aS_t^\varepsilon + b}{\sqrt{4ac - b^2}} \right)}{\sqrt{4ac - b^2}} - \frac{\rho V_t^\varepsilon}{K^\varepsilon\sigma} \end{cases}$

* Here r is the risk-free interest rate, q the dividend yield, X_t^ε , V_t^ε , $V_t^{\varepsilon,\gamma}$ and S_t^ε defined by (8), $\chi(V_t^{\varepsilon,\gamma}) := \int_0^\infty e^{-\gamma\varepsilon} \gamma V_t^{\varepsilon,\gamma} m(d\gamma)$, $K^\varepsilon = \varepsilon^{H-\frac{1}{2}}/\Gamma(H+1/2)$ the with the perturbation parameter $0 < \varepsilon \ll 1$ and the Hurst parameter $H \in (0, 1/2)$.

Example 5.1 (European and barrier options) *The value of European and barrier options can be calculated by Algorithm 4.1 and Algorithm 4.2. Due to the independence between the auxiliary process X_t^ε and the volatility process V_t^ε , the following fast algorithm can be used to speed up calculations.*

Algorithm 5.1 (A fast 2 dimensional CTMC algorithm for European and barrier options)

Under the setting that $g(s^\varepsilon) - \rho f(v^\varepsilon) = x^\varepsilon = x_i^\varepsilon$, $v^\varepsilon = v_\ell^\varepsilon$,

$$\begin{aligned}
& \mathbb{E} [\phi(S_T^\varepsilon, V_T^\varepsilon) | S_t^\varepsilon = s^\varepsilon, V_t^\varepsilon = v^\varepsilon] \\
& \approx \mathbb{E} \left[\phi(g^{-1}(\tilde{X}_t^\varepsilon + \rho f(\tilde{V}_t^\varepsilon)), \tilde{V}_t^\varepsilon) | \tilde{X}_t^\varepsilon = x_i^\varepsilon, \tilde{V}_t^\varepsilon = v_\ell^\varepsilon \right] \\
& = \sum_{j=1}^M (e^{\mathbf{Q}T})_{\ell,j} \mathbb{E} \left[\phi(g^{-1}(\tilde{X}_T^\varepsilon + \rho f(\tilde{V}_T^\varepsilon)), v_j^\varepsilon) | \tilde{X}_t^\varepsilon = x_i^\varepsilon \right] \\
& = \sum_{j=1}^M (\exp(\mathbf{Q}(T-t)))_{\ell,j} \times \mathbf{e}_i \cdot \exp(\mathbf{\Lambda}_\ell(T-t)) \cdot \mathbf{\Phi}_\ell,
\end{aligned} \tag{19}$$

where \mathbf{e}_i is a $1 \times N$ vector with all entries equal to 0 except that the i th entry is equal to 1, \mathbf{Q} is given by (11), $\mathbf{\Lambda}_\ell$ is given by (13), and the payoff vector $\mathbf{\Phi}_\ell$ is a $N \times 1$ vectors with elements $(\mathbf{\Phi}_\ell)_i = \phi(g^{-1}(x_i^\varepsilon + \rho f(v_\ell^\varepsilon)), v_\ell^\varepsilon)$, for $\ell \in \mathcal{M}$, $i \in \mathcal{N}$. For European option, we have

$$\phi(g^{-1}(x_i^\varepsilon + \rho f(v_\ell^\varepsilon))) = \begin{cases} (g^{-1}(x_i^\varepsilon + \rho f(v_\ell^\varepsilon)) - D)^+ & \text{for a call,} \\ (D - g^{-1}(x_i^\varepsilon + \rho f(v_\ell^\varepsilon)))^+ & \text{for a put.} \end{cases}$$

and for barrier option, there is

$$\phi(g^{-1}(x_i^\varepsilon + \rho f(v_\ell^\varepsilon))) = \begin{cases} (g^{-1}(x_i^\varepsilon + \rho f(v_\ell^\varepsilon)) - D)^+ \mathbf{1}_{\{L < g^{-1}(x_i^\varepsilon + \rho f(v_\ell^\varepsilon)) < U\}} & \text{for a call,} \\ (D - g^{-1}(x_i^\varepsilon + \rho f(v_\ell^\varepsilon)))^+ \mathbf{1}_{\{L < g^{-1}(x_i^\varepsilon + \rho f(v_\ell^\varepsilon)) < U\}} & \text{for a put.} \end{cases}$$

Remark 5.1 *When applying the CTMC method to a two-dimensional problem, the two-dimensional probability transition matrix is usually converted into a large matrix (see Song et al. (2016) and Xi et al. (2019)). In this way, we need to calculate the matrix exponential where the exponent is a $NM \times NM$ matrix. This is time consuming, and requires a lot of computer storage space for intermediate inputs. Since the two stochastic processes are separated by Lemma 3.1, we only need to compute $N \times N$ matrices M times using our method. This greatly reduces the unnecessary calculation, reduces the computer storage space, and improves the operation efficiency. See Figure 1 for the comparison of actual operation efficiency.*

Table 4 shows that with the decrease of ε , the European options prices under RSLV models will converge to the benchmarks. For barrier options, there are similar results, which are listed in Table 5. These results show the accuracy of the semimartingale and CTMC approximation algorithm. From Figures 2 and 3, we see that for a fixed ε , increasing the number of CTMC grids will make the relative error between the calculated results and the benchmark gradually decrease. It is worth mentioning that, for fixed $N = M = 100$, the average CPU times to calculate the European and barrier option prices are respectively 0.18 and 0.20 seconds. This shows the very high efficiency of our algorithm.

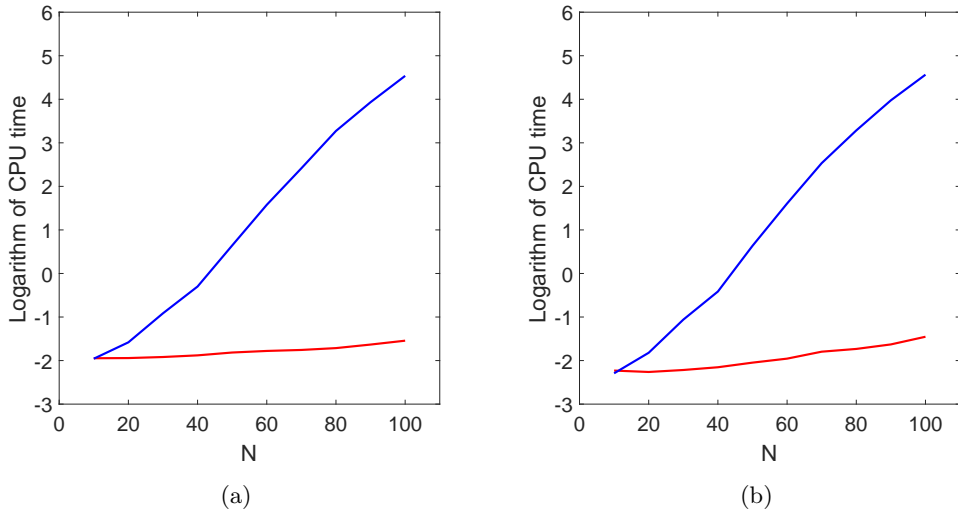


Figure 1: The plot of the number of grid points versus logarithmic of CPU times (seconds) for European (1(a)) and barrier (1(b)) options under rough Heston model. Here we set $M = N$. The blue lines in 1(a) and 1(b) are obtained by Algorithm 4.1 and 4.2, respectively. The red lines are obtained by Algorithm 5.1.

Table 4: European call option under the RSLV models.

ε	Relative Errors					
	R-H	R-4/2	R- α -H	R-SABR	R-H-SABR	R-Q-SLV
10^{-4}	4.71e-3	9.98e-3	5.76e-3	8.78e-3	4.21e-3	5.86e-3
10^{-5}	2.84e-3	9.68e-3	2.56e-3	3.81e-3	2.86e-3	4.53e-3
10^{-6}	2.07e-3	7.92e-3	1.22e-3	1.75e-3	2.32e-3	3.97e-3
10^{-7}	1.75e-3	7.55e-3	6.66e-4	8.84e-4	2.09e-3	3.44e-3
10^{-8}	1.61e-3	6.57e-3	4.34e-4	5.25e-4	1.99e-3	2.98e-3
benchmark	6.0545	0.0362	6.0001	4.9269	6.0018	6.0000

* Here “R-H”, “R-4/2”, “R- α -H”, “R-SABR”, “R-H-SABR”, “R-Q-SLV” represent “rough Heston”, “rough 4/2 model”, “rough α -Hyper”, “rough SABR”, “rough Heston-SABR”, “rough quadratic SLV” models respectively. Benchmarks are obtained by fast simulation algorithm based on the Monte Carlo method in Ma and Wu (2021) with 10^5 simple paths, and they take about 610.86 seconds on average. The results in the table are calculated with $N = M = 100$ via Algorithm 5.1, and take only 0.18 seconds on average.

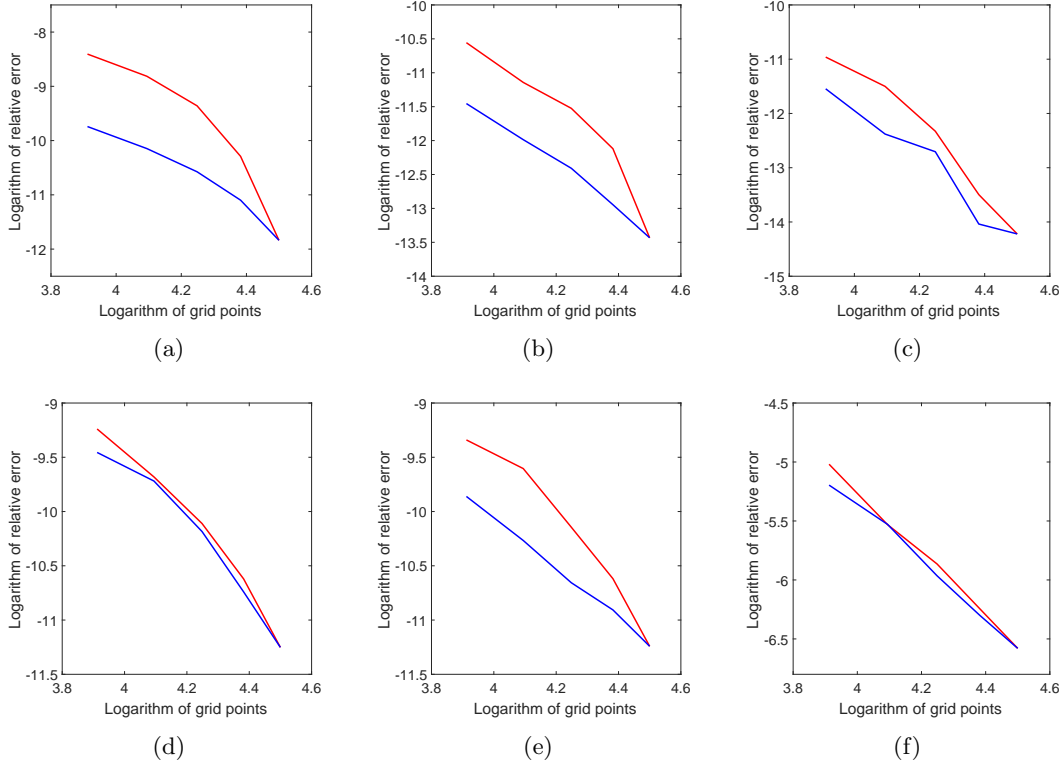


Figure 2: The logarithmic plot of the number of grid points versus relative error for European options under rough stochastic local volatility models via Algorithm 5.1. Figures 2(a), 2(b), 2(c), 2(d), 2(e), 2(f) correspond to rough Heston, 4/2, α -Hyper, SABR, Heston-SABR, quadratic SLV models, respectively. The red lines are obtained by fixing $M = 90$, and then increasing the grid points of N from 50 to 90. The blue lines are obtained by fixing $N = 90$ and changing M . Here we take the prices obtained by $M = N = 100$, $\varepsilon = 10^{-10}$ as the benchmarks to calculate relative errors.

Table 5: Barrier call option under the RSLV models.

ε	Relative Errors					
	R-H	R-4/2	R- α -H	R-SABR	R-H-SABR	R-Q-SLV
10^{-4}	4.21e-3	7.52e-3	3.54e-3	1.51e-3	2.84e-3	9.34e-3
10^{-5}	2.86e-3	6.18e-3	1.68e-3	7.42e-4	2.07e-3	5.76e-3
10^{-6}	2.32e-3	5.63e-3	9.07e-4	4.21e-4	1.75e-3	2.56e-3
10^{-7}	2.08e-3	5.40e-3	5.86e-4	2.88e-4	1.61e-3	1.22e-3
10^{-8}	1.99e-3	5.30e-3	4.53e-4	2.32e-4	1.56e-3	6.66e-4
benchmark	6.0492	0.0345	5.9753	4.8099	6.0000	5.9814

* Here "R-H", "R-4/2", "R- α -H", "R-SABR", "R-H-SABR", "R-Q-SLV" represent "rough Heston", "rough 4/2 model", "rough α -Hyper", "rough SABR", "rough Heston-SABR", "rough rough quadratic SLV" models respectively. Benchmarks are obtained by fast simulation algorithm based on Monte Carlo method in [Ma and Wu \(2021\)](#) with 10^5 simple paths, and they take about 800.13 seconds on average. The results in the table are calculated with $N = M = 100$ via Algorithm 5.1, and they take only 0.20 seconds on average.

Table 6: American call option under the RSLV models.

ε	Relative Errors					
	R-H	R-4/2	R- α -H	R-SABR	R-H-SABR	R-Q-SLV
10^{-4}	9.82e-3	9.99e-3	8.53e-3	9.25e-3	7.41e-3	8.88e-3
10^{-5}	6.73e-3	9.36e-3	6.25e-3	8.66e-3	5.55e-3	7.21e-3
10^{-6}	4.21e-3	8.95e-3	4.33e-3	7.99e-3	4.21e-3	6.85e-3
10^{-7}	3.75e-3	8.50e-3	3.28e-3	7.21e-3	3.48e-3	6.01e-3
10^{-8}	2.88e-3	8.12e-3	2.79e-3	6.54e-3	3.01e-3	5.75e-3
benchmark	6.0635	0.0418	6.1111	6.0000	6.4410	7.1658

* Here "R-H", "R-4/2", "R- α -H", "R-SABR", "R-H-SABR", "R-Q-SLV" represent "rough Heston", "rough 4/2 model", "rough α -Hyper", "rough SABR", "rough Heston-SABR", "rough rough quadratic SLV" models respectively. Benchmarks obtained by fast simulation algorithm based on least squares Monte Carlo method with 10^5 simple paths, and they take about 875.26 seconds on average. The results in the table are calculated with $N = M = 100$ via Algorithm 4.3, and they take 91.24 seconds on average.

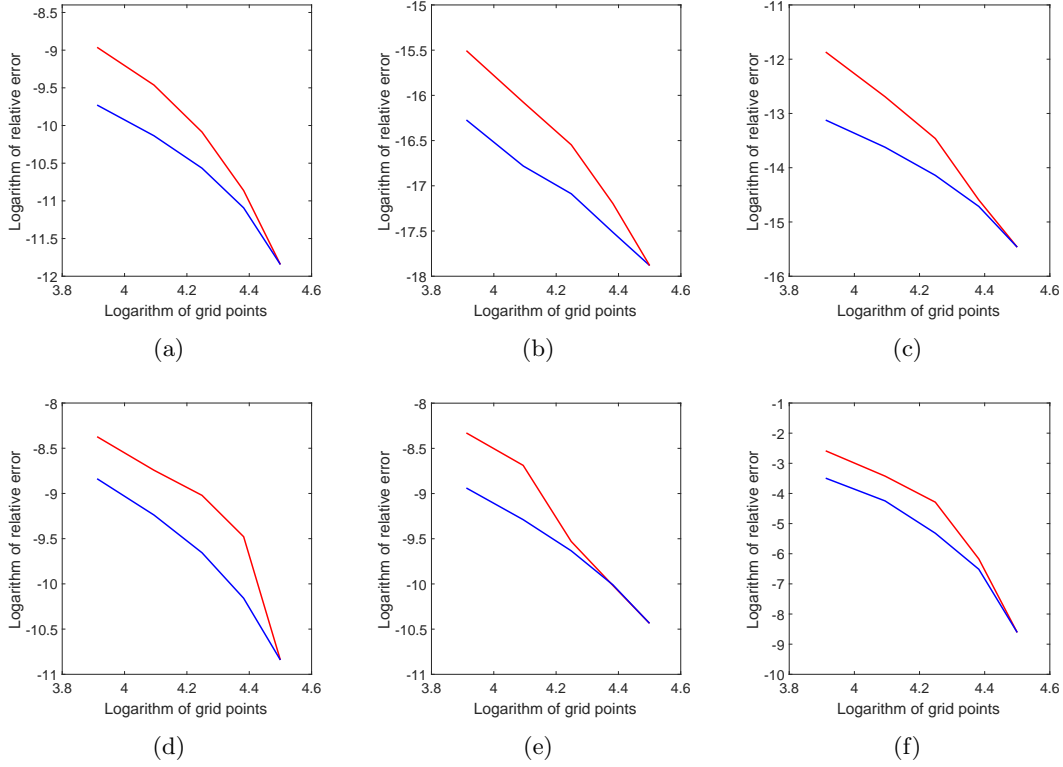


Figure 3: The logarithmic plot of the number of grid points versus relative error for barrier options under rough stochastic local volatility models via Algorithm 5.1. Figures 3(a), 3(b), 3(c), 3(d), 3(e), 3(f) correspond to rough Heston, 4/2, α -Hyper, SABR, Heston-SABR, quadratic SLV models, respectively. The red lines are obtained by fixing $M = 90$, and then increasing the grid points of N from 50 to 90. The blue ones are obtained by fixing $N = 90$ and changing M . Here we take the prices obtained by $M = N = 100$, $\varepsilon = 10^{-10}$ as the benchmarks to calculate relative errors.

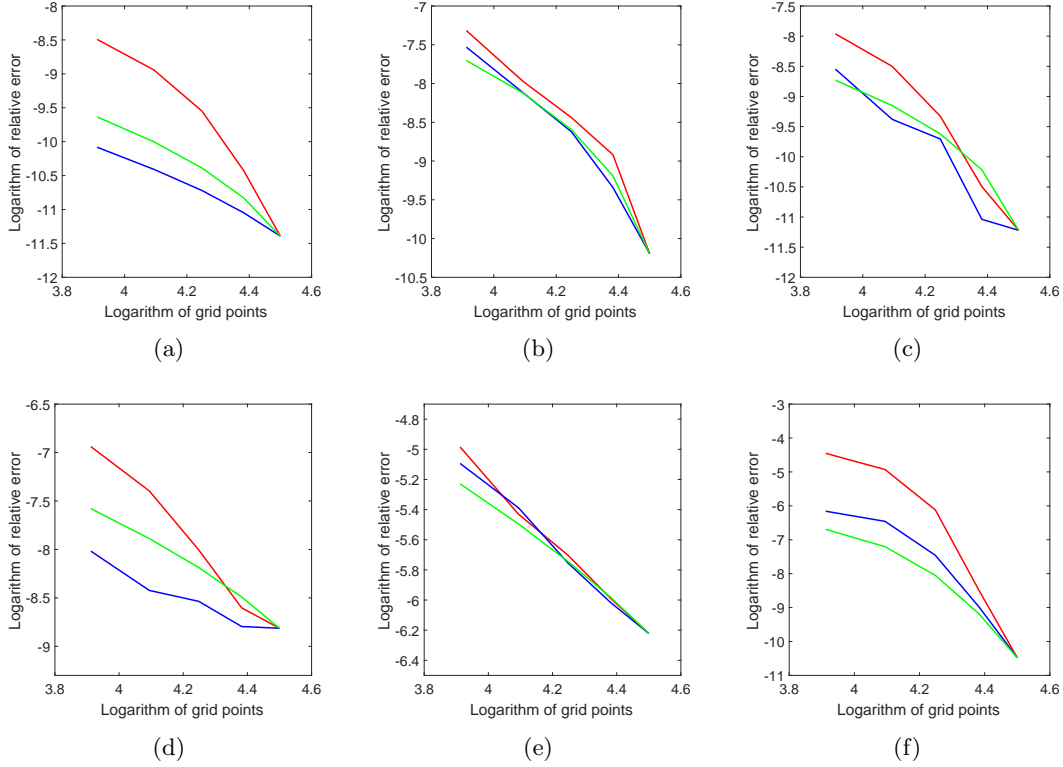


Figure 4: The logarithmic plot of the number of grid points versus relative error for American options under rough stochastic local volatility models via Algorithm 4.3. Figures 4(a), 4(b), 4(c), 4(d), 4(e), 4(f) correspond to rough Heston, 4/2, α -Hyper, SABR, Heston-SABR, quadratic SLV models, respectively. The red lines are obtained by fixing $n = M = 90$, and then increasing the grid points of N from 50 to 90. The blue ones are obtained by fixing $n = N = 90$ and changing M , and the green ones are obtained by fixing $N = M = 90$ and changing n . Here we take the prices obtained by $n = N = M = 100$, $\varepsilon = 10^{-10}$ as the benchmarks to calculate relative errors.

Example 5.2 (American option) *In this example, we use Algorithm 4.3 to calculate the price of American options under the six models listed in the Table 2.*

Table 6 shows that with the decrease of ε , the American options prices under RSLV models will converge to the benchmark. This demonstrates the accuracy of the semimartingale and CTMC approximation algorithm. In addition to showing the convergence results of CTMC grid points N and M , Figure 4 also shows the influence of the change in grid points on the relative error in the time direction. These results show the convergence of Algorithm 4.3. Since the value of the American option depends on the optimal stopping time, the fast Algorithm 5.1 is not available. However, the average CPU time to calculate American option prices is 91.24 seconds, which is significantly less than the least squares Monte Carlo method. Moreover, compared with Table 4 in Goudenège et al. (2020), which spend a significant amount of time to price American options under the simple Bergomi model, Algorithm 4.3 is clearly more effective and widely applicable for pricing American options under general rough stochastic local volatility models.

6 Conclusions

In this paper, we first propose a perturbation approach to approximate the rough stochastic local volatility model by a perturbed stochastic local volatility model, which is a semimartingale. After further expressing it as a Markovian form, we propose a continuous-time Markov chain approximation approach to derive the semi-explicit expressions of European, barrier and American options prices. The approximate expression obtained by this method is proved to converge to the solution of the original option pricing problem under the RSLV model. Numerical experiments demonstrate the accuracy and very high efficiency of the method for several RSLV models, including rough Heston and rough SABR models, etc.

References

- Abi Jaber, E., Larsson, M. and Pulido, S. (2019). Affine volterra processes. *The Annals of Applied Probability*, 29, 3155–3200.
- Abi Jaber, E. and El Euch, O. (2019). Markovian structure of the Volterra Heston model. *Statistics and Probability Letters*, 149, 63–72.
- Abi Jaber, E. and El Euch, O. (2019). Multifactor approximation of rough volatility models. *SIAM Journal on Financial Mathematics*, 10, 309–349.
- Alfonsi, A. and Kebaier, A. (2021). Approximation of Stochastic Volterra Equations with kernels of completely monotone type. arXiv preprint arXiv:2102.13505.
- Bayer, C., Ben Hammouda, C. and Tempone, R. (2020). Hierarchical adaptive sparse grids and quasi-Monte Carlo for option pricing under the rough Bergomi model. *Quantitative Finance*, 20, 1457–1473.
- Bayer, C. and Breneis, S. (2021). Markovian approximations of stochastic Volterra equations with the fractional kernel. arXiv preprint arXiv:2108.05048.
- Bayer, C., Friz, P. and Gatheral, J. (2016). Pricing under rough volatility. *Quantitative Finance*, 16, 887–904.
- Bayer, C., Friz, P.K., Gassiat, P., Martin, J. and Temper, B. (2020). A regularity structure for rough volatility. *Mathematical Finance*, 30, 782–832.
- Cai, N., Song, Y. and Kou, S. (2015). A general framework for pricing Asian options under Markov processes. *Operations Research*, 63, 540–554.
- Callegaro, G., Grasselli, M. and Pages, G. (2021). Fast hybrid schemes for fractional Riccati equations (rough is not so tough). *Mathematics of Operations Research*, 46, 221–254.
- Carmona, P., Coutin, L. and Montseny, G. (2000). Approximation of some Gaussian processes. *Statistical Inference for Stochastic Processes*, 3, 161–171.
- Cohen, S.N. and Elliott, R.J. (2015). *Stochastic Calculus and Applications (Vol. 2)*. New York: Birkhäuser.
- Cui, Z., Kirkby, J.L. and Nguyen, D. (2018). A general valuation framework for SABR and stochastic local volatility models. *SIAM Journal on Financial Mathematics*, 9, 520–563.
- Cui, Z., Kirkby, J.L. and Nguyen, D. (2019). Continuous-time Markov chain and regime switching approximations with applications to options pricing. In *Modeling, stochastic control, optimization, and applications* (pp. 115–146). Springer, Cham.
- Da Fonseca, J. and Martini, C. (2016). The α -hypergeometric stochastic volatility model. *Stochastic Processes and their Applications*, 126, 1472–1502.
- Dandapani, A., Jusselin, P. and Rosenbaum, M. (2021). From quadratic Hawkes processes to super-Heston rough volatility models with Zumbach effect. *Quantitative Finance*, 1–13.
- Dung, N.T. (2011). Semimartingale approximation of fractional Brownian motion and its applications. *Computers and Mathematics with Applications*, 61, 1844–1854.
- Durrett, R. (2018). *Stochastic Calculus: A Practical Introduction*. CRC press.
- El Euch, O., Fukasawa, M. and Rosenbaum, M. (2018). The microstructural foundations of leverage effect and rough volatility. *Finance and Stochastics*, 22, 241–280.
- El Euch, O., Gatheral, J. and Rosenbaum, M. (2019). Roughening Heston. *Risk*, 84–89.
- El Euch, O. and Rosenbaum, M. (2019). The characteristic function of rough Heston models. *Mathematical Finance*, 29, 3–38.
- Eriksson, B. and Pistorius, M.R. (2015). American option valuation under continuous-time markov chains. *Advances in Applied Probability*, 47, 378–401.

- Ethier, S.N. and Kurtz, T.G. (2009). *Markov Processes: Characterization and Convergence*. John Wiley and Sons.
- Forde, M., Smith, B. and Viitasaari, L. (2021). Rough volatility, CGMY jumps with a finite history and the Rough Heston model-small-time asymptotics in the $k\sqrt{t}$ regime. *Quantitative Finance*, 21, 541–563.
- Forde, M., Gerhold, S. and Smith, B. (2021). Small-time, large-time, and asymptotics for the Rough Heston model. *Mathematical Finance*, 31, 203–241.
- Forde, M. and Zhang, H. (2017). Asymptotics for rough stochastic volatility models. *SIAM Journal on Financial Mathematics*, 8, 114–145.
- Fukasawa, M., Takabatake, T. and Westphal, R. (2019). Is volatility rough?. arXiv preprint arXiv:1905.04852.
- Gatheral, J., Jaisson, T. and Rosenbaum, M. (2018). Volatility is rough. *Quantitative Finance*, 18, 933–949.
- Goudenège, L., Molent, A. and Zanette, A. (2020). Machine learning for pricing American options in high-dimensional Markovian and non-Markovian models. *Quantitative Finance*, 20, 573–591.
- Grasselli, M. (2017). The 4/2 stochastic volatility model: a unified approach for the Heston and the 3/2 model. *Mathematical Finance*, 27, 1013–1034.
- Guenoun, H., Jacquier, A., Roome, P. and Shi, F. (2018). Asymptotic behavior of the fractional Heston model. *SIAM Journal on Financial Mathematics*, 9, 1017–1045.
- Hagan, P.S., Kumar, D., Lesniewski, A.S. and Woodward, D.E. (2002). Managing smile risk. *Wilmott Magazine*, 1, 84–108.
- Harms, P. (2019). Strong convergence rates for Markovian representations of fractional Brownian motion. arXiv preprint arXiv:1902.01471.
- Heston, S.L. (1993). A closed-form solution for options with stochastic volatility with applications to bond and currency options. *The Review of Financial Studies*, 6, 327–343.
- Horvath, B., Jacquier, A. and Tankov, P. (2020). Volatility options in rough volatility models. *SIAM Journal on Financial Mathematics*, 11, 437–469.
- Hull, J. and White, A. (1987). The pricing of options on assets with stochastic volatilities. *The Journal of Finance*, 42, 281–300.
- Jaisson, T. and Rosenbaum, M. (2016). Rough fractional diffusions as scaling limits of nearly unstable heavy tailed Hawkes processes. *The Annals of Applied Probability*, 26, 2860–2882.
- Kushner, H.J. and Dupuis, P.G. (2001). *Numerical Methods for Stochastic Control Problems in Continuous Time*. Springer Science and Business Media.
- Lewis A. (2000), *Option Valuation under Stochastic Volatility*, Finance Press.
- Lipton, A. (2002). The vol smile problem. *Risk Magazine*, 15, 61–65.
- Livieri, G., Mouti, S., Pallavicini, A. and Rosenbaum, M. (2018). Rough volatility: evidence from option prices. *IISE transactions*, 50, 767–776.
- Ma, J. and Wu, H. (2021). A fast algorithm for simulation of rough volatility models, *Quantitative Finance*, forthcoming, DOI:10.1080/14697688.2021.1970213
- Ma, J., Yang W. and Cui Z. (2021). Convergence analysis for continuous-time Markov chain approximation of stochastic local volatility models: option pricing and Greeks. *Journal of Computational and Applied Mathematics*, forthcoming, DOI: 10.1016/j.cam.2021.113901
- McCrickerd, R. and Pakkanen, M.S. (2018). Turbocharging Monte Carlo pricing for the rough Bergomi model. *Quantitative Finance*, 18, 1877–1886.

- Mijatović, A. and Pistorius, M. (2013). Continuously monitored barrier options under Markov processes. *Mathematical Finance*, 23, 1–38.
- Okseidal, B. (2013). *Stochastic differential equations: an introduction with applications*. Springer Science and Business Media.
- Prigent, J.L. (2003). *Weak Convergence of Financial Markets*. Springer, Berlin, Heidelberg.
- Quecke, S. (2007). Efficient numerical methods for pricing American options under Lévy models. Diss. Verlag nicht ermittelbar.
- Richard, A., Tan, X. and Yang, F. (2021). On the discrete-time simulation of the rough Heston model. arXiv preprint arXiv:2107.07835.
- Song, Y., Cai, N. and Kou, S. (2016). A unified framework for options pricing under regime switching models. Available at SSRN 3310365.
- Stein, E.M. and Stein, J.C. (1991). Stock price distributions with stochastic volatility: an analytic approach. *The Review of Financial Studies*, 4, 727–752.
- Tavella, D. and Randall, C. (2000). *Pricing Financial Instruments: The Finite Difference Method*. Wiley, New York.
- Van der Stoep, A.W., Grzelak, L.A. and Oosterlee, C.W. (2014). The Heston stochastic-local volatility model: efficient Monte Carlo simulation. *International Journal of Theoretical and Applied Finance*, 17, 1–30.
- Veraar, M. (2012). The stochastic Fubini theorem revisited. *Stochastics An International Journal of Probability and Stochastic Processes*, 84, 543–551.
- Xi, Y., Ding, K. and Ning, N. (2019). Simultaneous two-dimensional continuous-time Markov chain approximation of two-dimensional fully coupled Markov diffusion processes. Available at SSRN 3461115.